Construction and Building Materials 251 (2020) 118976

Contents lists available at ScienceDirect

Construction and Building Materials

journal homepage: www.elsevier.com/locate/conbuildmat

Evaluation of the 12–24 mm basalt fibers and boron waste on reinforced metakaolin-based geopolymer

Nawar Ali [a], Orhan Canpolat [a,*], Yurdakul Aygörmez [a], Mukhallad M. Al-Mashhadani [b]

[a] Yildiz Technical University, Civil Engineering Department, Davutpasa Campus, Istanbul, Turkey
[b] Istanbul Gelisim University, Civil Engineering Department, Avcilar Campus, Istanbul, Turkey

HIGHLIGHTS

- Basalt fiber reinforced metakaolin geopolymer composites were fabricated.
- Metakaolin was partially replaced with colemanite waste.
- Influence of Elevated tepmeratures, freeze-thaw and sulfuric acid were investigated.

ARTICLE INFO

Article history:
Received 23 December 2019
Received in revised form 13 February 2020
Accepted 1 April 2020
Available online 8 April 2020

Keywords:
Geopolymer
Metakaolin
Boron
Basalt fiber
Abrasion resistance
High temperature
Freezing-thawing
Hydrosulfuric acid

ABSTRACT

Concerning sustainability and recycling considerations, geopolymers have recently raised as one of the most active alternatives to the current cement-based composites, in addition to that, the existence of fibers in any binding matrix yields a significant improvement in the behavior of the matrix. On the other hand, using waste materials in the binding matrices fulfills one of the main aims of sustainability, namely reusing wastes. In this concern, the previous research attempts focused on the effect of using fibers and wastes separately and hence using them together in one matrix is not clearly highlighted. The main objective of this study was to examine the engineering properties of metakaolin-based geopolymer mortars in the case of colemanite substitution up to 30% and basalt fiber of different lengths. In the 10 series produced, firstly 7th day and 28th day compressive and flexural strengths, UPV, abrasion resistance test, porosity, unit weight, and water absorption results were examined. As the durability tests, 90 cycles of freezing-thawing between −20 and +20 °C, high-temperature tests of 250, 500 and 750 °C were applied. Also, geopolymer samples were exposed to 10% Hydrosulfuric Acid (H_2SO_4) for 3 months. Scanning Electron Microscopy (SEM), X-ray Diffraction (XRD), Fourier Transform Infrared Spectroscopy (FT-IR) and Thermogravimetric/Differential Thermal Analysis (TGA-DTA) analyses were performed at the end of the durability tests. The results showed that in the case of 10% colemanite substitution, it increased the compressive strength results and lowered it at higher rates. With a colemanite substitution of 10%, the compressive strength results of 28 days increased by 1.71%, and in the case of 20% and 30% colemanite substitution, there was a decrease in the compressive strength of 13.64% and 26.99%, respectively. The compressive strength results showed that 24 mm long basalt fiber reinforced samples had better results than 12 mm long basalt fiber reinforced samples. It was seen that geopolymer specimens maintain stability in freezing-thawing, elevated temperatures, and sulfuric acid effects.

1. Introduction

Metakaolin is produced with calcification of kaolin between 500 and 1000 °C and has high pozzolanic properties [1]. It is a binder material that provides a strong reaction with alkali solutions and increases strength [2–4]. Davidovits stated that geopolymer composites produced using metakaolin and slag gave the best results for engineering characteristics [5]. The geopolymerization reaction produced using metakaolin depends on the metakaolin's type, the concentration and activator's amount and the curing system applied [6–8]. Much research has been done about metakaolin based geopolymers [9–13].

Geopolymers are generally alternative to Portland cement and have important strength and durability properties [14–17]. Moreover, it is a composite material which has lower permeability than

* Corresponding author.
E-mail address: canpolat@yildiz.edu.tr (O. Canpolat).

https://doi.org/10.1016/j.conbuildmat.2020.118976
0950-0618/

Portland concrete and has a high resistance to heat and can be cured rapidly [18]. For a geopolymer, it is beneficial to utilize different waste materials besides metakaolin.

Pelisser et al. [19] examine the flexural modulus, hardness, flexural and compressive strengths, elasticity modulus and microstructure properties of geopolymer mortars produced by metakaolin. The results showed that geopolymer mortars were superior to portland cement mortars. It also had higher performance in terms of tensile strength and deformation capacity.

Rovnanik [20] investigated the effect of different curing temperatures such as 10, 20, 40, 60 and 80 °C and curing times on the geopolymerization. The results were compared in terms of microstructure, pore distribution, and flexural and compressive strengths. The study showed that the pore size changes with the curing temperature affected the mechanical properties. It has shown that geopolymerization can be followed by Infrared Spectroscopy analysis.

Zhang et al. [21] produced the metakaolin and F class fly ash-based geopolymer composites for fire resistance. The strength results were analyzed with a high-temperature effect. An alternative product against elevated temperatures was presented according to the strength results and thermogravimetric analysis.

Lahoti et al. [22] investigated the effect of Al/Na, Si/Al, H_2O/Na_2O and water/binding materials ratios on the compressive strength properties. While the most important factor in the Ordinary Portland cement samples is known to be water/binder ratio, the most important factor for geopolymer samples is Si/Al.

Meanwhile, the use of waste materials is one of the important procedures in this field, the world's largest boron mine deposits are in Turkey. Approximately 1.72 million tons of boron products can be fabricated in Turkey [23,24]. One of the most important boron products is colemanite. Colemanite is called a calcium borate mineral and has a hardness value between 4 and 4.5. Also, the B_2O_3 ratio of pure colemanite is approximately 51%. In the stages of production, many by-products are fabricated. These by-products that generate waste materials cause environmental pollution. In particular, colemanite waste leads to pollution of underwater resources. Colemanite waste is utilized as a mineral for the cement industry to prevent or minimize this situation [24,–25]. Kula et al. examined the contribution of colemanite to the mechanical properties of the mortar produced using fly ash and bottom ash. The most important parameter is the B_2O_3 content [26]. It has been found that colemanite waste has a positive effect on the mechanical properties when it is used as a mineral additive up to 10% by weight [27].

Djobo et al. [28] examined the mechanical and durability properties of volcanic ash-based geopolymer composites produced at curing temperatures of 27 and 80 °C under aggressive ambient conditions. Geopolymer samples were exposed to 5% sulfuric acid. Microstructural analyses of geopolymer samples were examined after acid effect and the gypsum formation, a secondary phase, was detected by the reaction of calcium present in the geopolymer gel with sulfuric acid. Low-temperature cured samples have increased the acid resistance of Na-rich gel.

Ariffin et al. [29] investigated the strength of geopolymer concrete by exposing a 2% sulfuric acid solution to samples produced using palm oil and pulverized fuel ash as a binder material. Also, concrete produced using OPC was used for comparison. Comparing the results, the geopolymer's stable aluminosilicate structure showed better performance against sulfuric acid.

Zhang et al. [30] examined the residual flexural and compressive strengths and microstructural analyzes by exposing the samples to sulfuric acid for up to 120 days with red mud and fly ash-based geopolymers. OPC was used for comparison purposes and it was concluded that the main cause of mechanical deterioration was depolymerization and delamination in the geopolymer gel. It was found that heavy metal concentrations in geopolymer samples exposed to sulfuric acid were lower than the limit values in terms of soil pollution. Mehta et al. [31] investigated the compressive strength, deterioration and weight loss by applying a 2% sulfuric acid solution to samples produced using fly-ash based geopolymer concrete with OPC (10%, 20%, 30%) because of its high calcium content. The use of substitutes increased sulfuric acid resistance by up to 10%, while maximum degradation and lowest values were obtained at the 30% substitution.

D. Shen et al.[32] examined the effect of using fly ash as a partially replaced material in high-performance concrete (HPC), they tested the effect of some mechanical and long term properties such as autogenous shrinkage and restrained stress on the behavior of the fabricated samples. They concluded that adding fly ash could contribute to enhancing the performance of the specimens under the conducted tests. Yunsheng et al. [33] applied a 20-cycle of freezing-thawing to the geopolymer samples fabricated using polyvinyl alcohol fiber. Hardness and impact strength tests indicated no effect after freezing-thawing which leads to a fact that the existence of PVA fibers could exhibit comparable results regarding impact properties.

Besides, the process of geopolymerization with the addition of fibers to the composites and thus the mechanical and durability performance can be improved. Many studies have been conducted in the concrete and cement sectors using different fibers such as carbon, glass, woven fabric, basalt, steel and wood [34–36]. Recently, these studies have shifted to geopolymer composites. Investigations were made by incorporating polyvinyl acetate, polypropylene, and polyvinyl alcohol fibers into the geopolymer matrix [37,38]. Dias and Thaumaturgo investigated the fracture toughness of geopolymer concrete using basalt fiber.

Arunagiri et al. [39] showed that the basalt fiber admixture positively affected the mechanical properties of geopolymer concrete and had the highest compressive strength contributing 2% by volume. It was also found that basalt fiber contributed significantly to keep the cracks and prevent sudden failures. When used at an optimum rate, it increases the tensile strength as well as the compressive strength. D. Shen et al. [40] conducted an experimental investigation on the bonding strength of geopolymer concrete reinforced with basalt fiber-reinforced polymer rebars under static loading. In general, their conclusions stated that reinforcing geopolymer composites with basalt fiber polymers was beneficial in terms of bonding strength and strain rates under the aforementioned loading.

The general withdrawn conclusions state the fact that the previous research attempts focused on the effect of fibers and wastes independently, in the light of this fact, no enough experimental studies were presented in order to clarify the combined effect of the aforementioned factors. In addition to that, focusing on the microstructural investigation for such studies needs to be inspected. The main categories which were concluded from the research gap and motivated this study mainly focused on fabricating geopolymeric composites using both fibers and waste materials, behavior under severe conditions, and investigation of strength and microstructural aspects.

Based on the reasons mentioned above, boron waste colemanite was added up to 30% as a substitution material to geopolymer composites produced differently. Also, 1% short (12 mm) and long (24 mm) basalt fibers were used to see the fiber effect on the geopolymer samples. The results of the 7 and 28 days compressive and flexural strength were investigated together with the unit weight, water absorption and porosity properties of the geopolymer composites. Compressive and flexural strengths, weight-loss and UPV results after the elevated temperature effect of 250, 500 and 750 °C were investigated. 90 cycles of freezing-thawing between −20 and +20 °C were applied. Also, geopolymer samples

were exposed to 10% Hydrosulfuric Acid (H_2SO_4) for 3 months. SEM, XRD, FT-IR and TGA-DTA analyses were performed after the durability tests. However, the weight loss results of geopolymer samples were measured as a result of the abrasion resistance test. SEM analysis of geopolymer samples with the effect of 250 and 500 °C was performed.

2. Experimental

For this paper, geopolymer composites were fabricated using metakaolin from Kaolin EAD and boron waste colemanite obtained from Eti Mine Company. Al_2O_3 + SiO_2 + Fe_2O_3 ratio is 97.18% of all chemical composition of binding metakaolin which has high pozzolanic activity. Its fine grains increase the degree of bond formation in geopolymerization. The slag obtained from Bolu Cement Company has participated in the mixture by 13%. The specific gravity of metakaolin is 2.52 g/cm^3 and the specific gravity of colemanite is 2.42 g/cm^3. The chemical properties of three different binders are described in detail in Table 1. Slag, colemanite, and metakaolin are shown with the abbreviations S, C and MK respectively.

The standard sand (BS EN 196-1) was obtained from Limak Group of Companies and was incorporated as aggregate into the geopolymer mixture. The sodium silicate and sodium hydroxide (8 M) were mixed and formed the activator solution.

For this paper, to analyze the fiber effect on the flexural strength after freezing-thawing, high temperature and sulfuric acid exposure and the weight loss after abrasion test, basalt fibers (12 mm and 24 mm) with two different lengths were added to the geopolymer mortars at a rate of 1% by volume. The properties of basalt fibers are given in Table 2. Also, short and long basalt fibers are shown with abbreviations of SBF and TBF, respectively.

The mixture of sodium hydroxide and silicate as the activator, metakaolin, slag and colemanite as binding materials and standard sand as aggregate was used for the geopolymer mixture. In preparing the mortar mixtures, the ratios are taken as 2/3 for silicate/binding material, 1/2.5 for binding material/sand and 1/3 for hydroxide/binding material. Previous studies were used during the preparation of the mixture [22,23,41–47]. Table 3 shows the amount of material required for the mixture.

To briefly summarize the geopolymer mortar mixture, the NaOH solution (8 M) prepared 24 h before the mixture was mixed with Na_2SiO_3 solution until a complete mix was obtained by a shaker. The main binder material metakaolin (450 g) was mixed with the activator solution (450 g) by a stirrer drill. The binding/activator ratio was taken as 1:1. A 13% slag was added to increase the amount of calcium in the geopolymerization reaction. In the final stage, the standard sand required for the mortar was added 2.5 times the binder ratio. The mortars produced were placed in prism and cube molds and subjected to vibration.

After keeping in the molds for 2 h, the samples were taken out from the molds and kept at the normal temperature for one day following. At the end of 24 h, they were put into the oven together with non-flammable oven bags. Temperature curing was applied at 60 °C for 3 days. During the heat curing, the bags reduced the evaporation of water in the geopolymeric matrices. It was removed from the oven at the end of 3 days and kept in the plastic storage containers until the experimental day. 28 days later, unit weight, water absorption, porosity, abrasion, freezing-thawing, high temperature, and sulfuric acid tests were carried out.

In this study, three different groups of geopolymer samples were produced with geopolymer samples prepared by using 100% metakaolin as a control sample. The first group was manufactured as fiberless by substituting up to 30% colemanite. The second group was obtained by adding 1% short basalt fiber to the first group and 1% of the tall basalt fiber was added in the third group. Basalt fiber and colemanite added mixing ratios are shown in Table 4.

For compressive strength cube samples (ASTM C 109 [48]) and flexural strength prism samples (ASTM C 348 [49]) were utilized. Following the abrasion test, the weight loss was determined. A rotary cutter abrasion machine was used for this experiment. By ASTM C944 [50], samples were eroded for 2 min with a load of 98 N and only in contact with cutters. For this experiment, cylinders with a diameter of 10 cm and a height of 7.5 cm were produced. This method was repeated three times in total for 2 min each time and the weight loss after each abrasion period was measured. The first abrasion and average abrasion loss values were calculated and the results were interpreted.

At the end of 28 days, 10 series of geopolymer mortar samples were applied at high temperatures of 250, 500 and 750° C. Samples were made dry in the drying oven at 100 °C for 24 h before testing. The temperature increment rate is set at 5 °C/min. Specimens were held at the target temperature for 60 min. After the test, samples were held in the drying oven for 24 h to prevent thermal shock. Also, freezing-thawing tests applied to the 10 series between −20 and +20 °C, which consisted of a total of 90 cycles. 1 cycle was set to 12 h at −20 °C and 12 h at +20 °C. Geopolymer mortar samples were kept in a plastic storage box at ambient temperature at the end of 28 days for 3 months in 10% sulfuric acid solutions. The specimens were held in the drying oven at 100 °C for 24 h for better absorption of the solutions. The solutions were renewed every month to maintain the solution concentration constant. The solution was placed in a box of 4 units for 1 unit sample volume. At the end of each month, samples were removed from the box for exposure to tests and allowed to dry at room temperature. Strength, UPV and weight loss were examined before and after all the tests. Visual inspection for the specimens was made.

3. Results and discussion

3.1. Strength results

The effect of basalt fiber and colemanite on compressive and flexural strength results were investigated. The strength results are given in Figs. 1 and 2. According to the results, colemanite substitution increased the compressive strength results by up to 10% and decreased in higher rates [46,47]. Colemanite wastes can be used up to 10% for geopolymer composites [26]. When boron minerals are used in the cemented system, a protective layer is formed round cement particles so the contact of water and cement particles is prevented with this protective layer. So this influence directly affects the cementitious materials' hydration mechanism

Table 1
The chemical properties for the metakaolin, colemanite waste, and slag.

Chemical properties %	SiO_2	Al_2O_3	Fe_2O_3	TiO_2	CaO	MgO	K_2O	Na_2O	B_2O_3	L.O.I.
MK	56.10	40.23	0.85	0.55	0.19	0.16	0.51	0.24	–	1.10
S	40.55	12.83	1.10	0.75	35.58	5.87	0.68	0.79	–	0.03
C	5.00	0.40	0.08	–	26.02	3.00	–	0.50	40.00	25.00

Table 2
The properties of basalt fibers.

Fiber type	Length (mm)	Diameter (μm)	Modulus of elasticity (GPa)	Elongation (%)	Tensile strength (MPa)	Density (g/cm^3)
SBF	12	13	89	3.15	4100	2.80
TBF	24	20	89	3.15	4800	2.80

Table 3
Mixing amounts of geopolymer mortar (g).

Metakaolin	Sand	Slag	NaOH (8 M)	Na_2SiO_3
450	1125	60	150	300

Table 4
Mixing percentages of geopolymer specimens (%).

Mix ID	Replacement ratio	MK
MK	–	100
10C	10	90
20C	20	80
30C	30	70
10C + SBF	10	90
20C + SBF	20	80
30C + SBF	30	70
10C + TBF	10	90
20C + TBF	20	80
30C + TBF	30	70

[51]. Also, boron additives increase the cement-based composites' strength results [52]. When the literature for boron minerals is examined, it can be seen that there is a critical threshold ratio for colemanite in terms of increasing strength. With the use of more than 10% colemanite, it is suggested that some anions and cations that cause unstable boron compounds have interfered with the cement activation mechanism in the system. Due to this situation, the decrease is thought to be seen.

With a 10% colemanite substitution, the 28-day compressive strength results increased by 1.71% while in the case of 20% colemanite substitution there was a decrease of 13.64% and in the case of 30% colemanite substitution, there was a decrease of 26.99%. Also, with the addition of basalt fiber and age increase, the compressive strength results of geopolymer samples increased and this was consistent with previous studies [47,53]. The increase in the number of fibers crossing the crack surface is one of the most important reasons that increase the flexural strength of mortar because it reduces the crack opening. Kayali [54], Zollo [55] reported that the basalt fiber's inclusion at different rates makes a contribution to the yield strength of the sample.

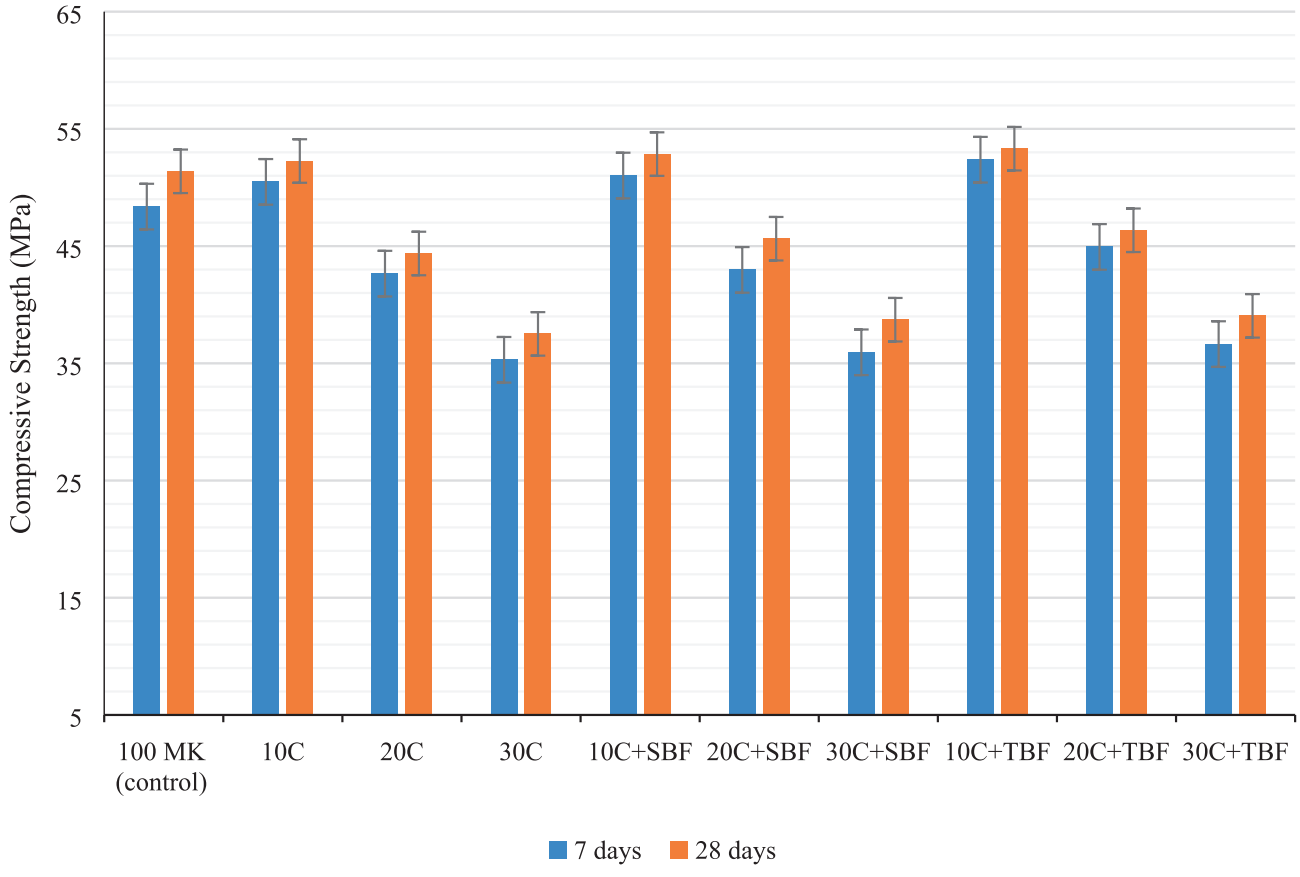

Fig. 1. Compressive strength values for the mixes.

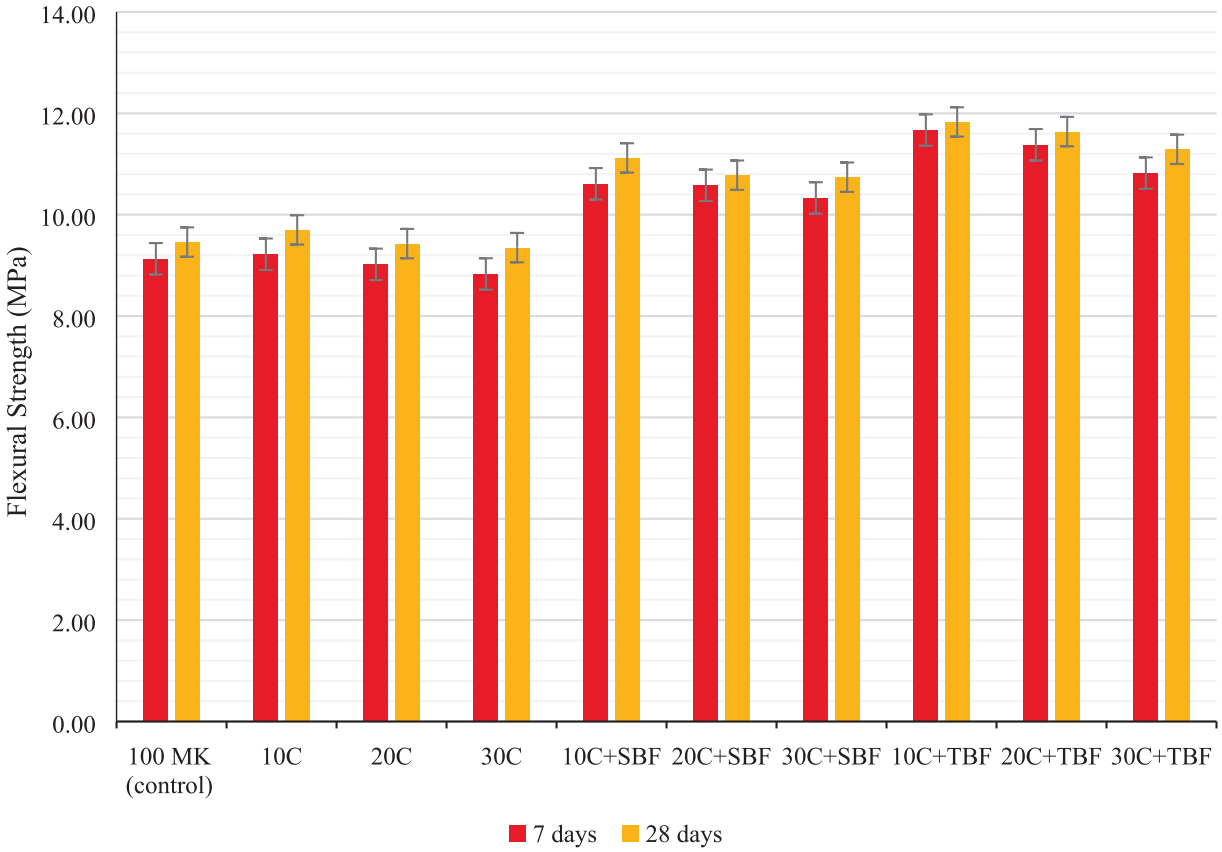

Fig. 2. Flexural strength values for the mixes.

When using 24-mm-long basalt fiber, a significant improvement was observed in the compressive strength results. This is consistent with previous studies [53]. The results showed that basalt fibers with a length of 24 mm had better results than basalt fibers with a length of 12 mm. This can be attributed to the effect that holding mortar particles more robustly is possible with a longer anchoring. Palchik [56] conducted compressive strength research using different basalt fibers of 24 mm and 12 mm length in cubic samples of 10x10x10 cm. 126 samples tested; while 18 samples were produced without fiber, in 108 samples basalt fibers were used. According to the results, the compressive strength results increased by 58% with basalt fibers of 24 mm and the compressive strength results increased by 25% in the samples using fiber with a length of 12 mm.

At the same time, the longer basalt fiber has a significant and positive effect on the flexural strength of the mortar sample. This is because longer fibers passing the crack zone can transfer the load more efficiently and redistribute the stress due to their ability to significantly reduce concrete cracks than short fibers. The longer the fibers transfer the stress, the longer the development of the crack; therefore, the flexural strengths that can be reached increases. The similar result was obtained by Jianxun Ma [57], who concluded that increasing the fiber content and length would increase the flexural strength.

In the case of basalt fiber with a length of 12 mm and a 10% colemanite substitution, the rate of increase in compressive strength of 28 days was 2.86%, while the decrease ratio for 20% colemanite substitution was 11.19% and the decrease ratio for 30% colemanite substitution was 24.64%. The addition of a 24 mm long basalt fiber and a 10% colemanite substitution yielded a 3.76% increase in compressive strength of 28 days, while the decrease ratio for 20% colemanite substitution was 9.79% and the decrease ratio for 30% colemanite substitution was 24%.

There was an increase in flexural strength results with %10 colemanite substitution and basalt fiber [46,47]. With a 10% colemanite substitution, the 28-days flexural strength was increased by 2.54%, with a 20% colemanite substitution flexural strength was decreased by 0.32% and with a 30% colemanite substitution flexural strength was decreased by 1.16%. In the case of basalt fiber with a length of 12 mm, the 28-day flexural strength results were increased by 17.55%, 13.95%, and 13.53%, respectively. In the case of the addition of a 24 mm long basalt fiber, the 28-day flexural

Table 5
Results for voids ratio, unit weight, and water absorption.

	Unit weight (g/cm^3)	Water absorption (%)	Voids ratio (%)
100 MK	2.36	25.8	14.78
10C	2.37	25.2	14.49
20C	2.39	23.9	14.15
30C	2.40	23.52	14.06
10C + SBF	2.43	24.06	13.74
20C + SBF	2.43	23.17	13.71
30C + SBF	2.45	22.38	13.13
10C + TBF	2.44	23.82	13.12
20C + TBF	2.46	22.71	12.73
30C + TBF	2.47	22.27	12.64

strength results were increased by 25.05%, 23.04%, and 19.34%, respectively.

3.2. Water absorption, unit weight, and voids ratio

The parameters of voids ratio, unit weight, and water absorption were investigated and given in Table 5 to see the change of physical behavior of the matrix formed in the geopolymer structure with the addition of basalt fiber and colemanite substitution.

Generally, the results showed a slight improvement in physical properties with the basalt fiber influence. This is due to the ability of the fiber to absorb water due to its characteristics. Thus, the water absorption rate of the matrix is reduced. The same condition was seen in the voids ratio. Neville [58] has shown that as the basalt fiber's ratios increase, the basalt fiber component is the lightest in the mixture and the effect for the unit weight is unnoticeable, resulting in a small increase for the concrete unit weight. Borhan [59] found similar results and indicated that the basalt fibers' influence was very small on unit weight. Also, when all the mixtures were examined, there was an improvement in physical properties as the colemanite substitution rate increased. It was found that the rate of water absorption and voids ratio decreased and the unit weight increased with increasing substitution rate.

The increase in unit weight with colemanite substitution was between 0.42% and 1.69%. When short basalt fiber was used, the increment ratios were between 2.97% and 3.81%. When long basalt fiber was used, the increment ratios were between 3.39% and 4.66%.

3.3. Ultrasonic pulse velocity

Ultrasonic pulse velocity test was applied to investigate the continuity of the geopolymer matrix structure with colemanite substitution and the addition of basalt fiber. The 7 and 28 days' results are given in Table 6. With the influence of basalt fiber and fiber length increase, the results increased. This was parallel to the increase in compressive strength [53]. However, the increase rate was lower than the compressive strength. Concerning the addition of fibers, the results of the mixes were close which shows that the homogeneity and the compactness of the matrix were not impressed with the fibers. Also, there was a slight increase in velocity between 7 and 28 days. As the colemanite waste substitutions increased, similar properties were observed to the strength results [46,47]. Al-mashhadani conducted similar research and found that there was a small improvement difference with the different fiber ratios in the same series as well as the same specimen at different ages [14].

For 10C samples, the results of 7 and 28 days increased by 1.51% and 0.90% respectively, while the results of 7 and 28 days for 20C samples were decreased by 4.10% and 5.11%, respectively. Also, the results of 7 and 28 days for 30C samples were decreased by 6.62% and 7.58%, respectively. 1.84% and 2.41% increase rates were observed with the effect of short and tall fibers in 10C samples in 28 days, respectively.

Table 6
Ultrasonic pulse velocity test results (m/s).

	7 Days	28 Days
100 MK	3367	3442
10C	3418	3473
20C	3229	3266
30C	3144	3181
10C + SBF	3429	3497
20C + SBF	3272	3321
30C + SBF	3183	3206
10C + TBF	3448	3512
20C + TBF	3313	3367
30C + TBF	3225	3254

3.4. Abrasion resistance

The weight loss resulting from the abrasion test is shown in Fig. 3. It was seen that the weight loss was reduced in the case of a 10% colemanite replacement. In the case of increasing substitution rates, an increase in weight loss was seen similar to the compressive strength.

When the average weight loss in the 10C sample decreased by 30.06%, the average weight loss increase rates in 20C and 30C samples were 22.70% and 33.13%, respectively. There was also important progress in weight loss after the abrasion test with basalt fiber. The decreases in weight loss in 10C + SBF and 10C + TBF samples were 52.15% and 63.80%, respectively. The results were consistent with previous results [14,46].

The findings of this study can be considered in accordance with previous studies [60]. Kabay conducted a study on the abrasion resistance of the concrete under the influence of basalt fiber. It was seen that adding basalt fiber improved abrasion resistance significantly for the concrete. Also, the increase in fiber content and length improved abrasion resistance.

3.5. The studied determination coefficients

An attempt has been made to investigate the results' conformity degree and find a correlation factor between the results. R^2 is called the correlation factor and the value of R^2 directly shows the results' conformity degree. When this value is greater than 0.8, it shows a very good correlation level. For this research, between the UPV and compressive strength and between the abrasion resistance and flexural strength were correlated. If a general result is obtained, a good degree of correlation was observed in Figs. 4 and 5. The correlation factor of the compressive strength-ultrasonic pulse velocity results for fiberless and fiber-reinforced samples was 0.96, while the correlation factor of the flexural strength-abrasion resistance results was 0.81.

To compare the present results with the previous findings, it is thought that the results of this study are consistent with them [14,46] in terms of the correlation between compressive strength-UPV and show more correlation between flexural strength-abrasion resistance relation.

3.6. High-temperature test

3.6.1. Strength results

Geopolymer specimens were examined under the influence of 250, 500 and 750 °C temperature. Also, to see the effect of short and long basalt fibers, they were put in the colemanite substitution mixtures by volume of 1%. The results of strength after the experiment were observed and compared with the pre-test results (Figs. 6 and 7). With the 500 °C temperature effect, the results have started to decrease significantly (Tables 7 and 8).

Geopolymer specimens showed a significant reduction in strength results due to dehydration and water evaporation with thermal reactions after 500 °C [61]. When the reduction rates of the flexural strength results were examined, it was determined that they were higher compared to compressive strength. The cause of this situation is the formation of imperfections such as the growth of porous structures and the spreading of cracks along with the temperature [62].

Test results usually showed a similar tendency to the specimens before elevated temperatures. The long and short basalt fibers reinforced specimens exhibited a lower strength loss than the control

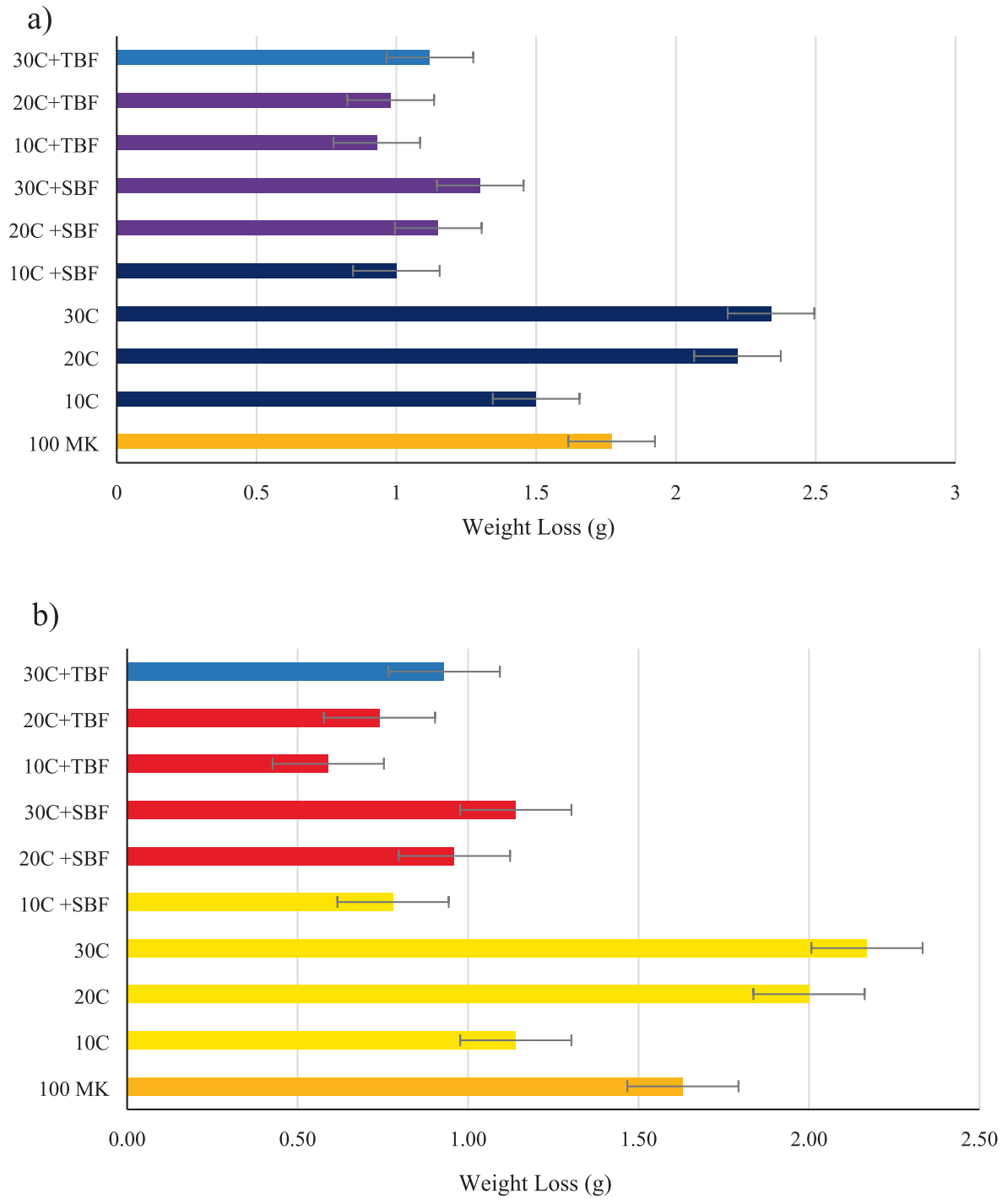

Fig. 3. Results of weight loss: a) 1st abrasion weight loss and b) average weight loss, respectively.

sample. Also, they showed a more standardized behavior than the control specimen. This is because the basalt fibers have preserved their shape and have not lost their mechanical integrity.

The fibers' desired engineering properties are connected to their crystalline phases' homogenous and thin distribution. The targeted microstructure properties can be acquired with a nucleating agent adding such as TiO_2, ZrO_2 or P_2O_5. Nevertheless, basalt rock doesn't need a core material, such as Fe_3O_4, along with melting, however, produces; therefore, nucleating agents provide benefits over alternative fibers required to achieve nearly the same microstructure [63,64]. After elevated temperatures, Kong et al. investigated the relative performance of the metakaolin and F-class fly ash-based geopolymers. They reported that the geopolymers were exposed to a strength loss after exposure to temperatures of 800 °C. Results indicated a 34% drop in the strength of using metakaolin after 300 °C [65].

The specimens' flexural strength results indicated a leaning to grow similar to the compressive strength results. Also, the

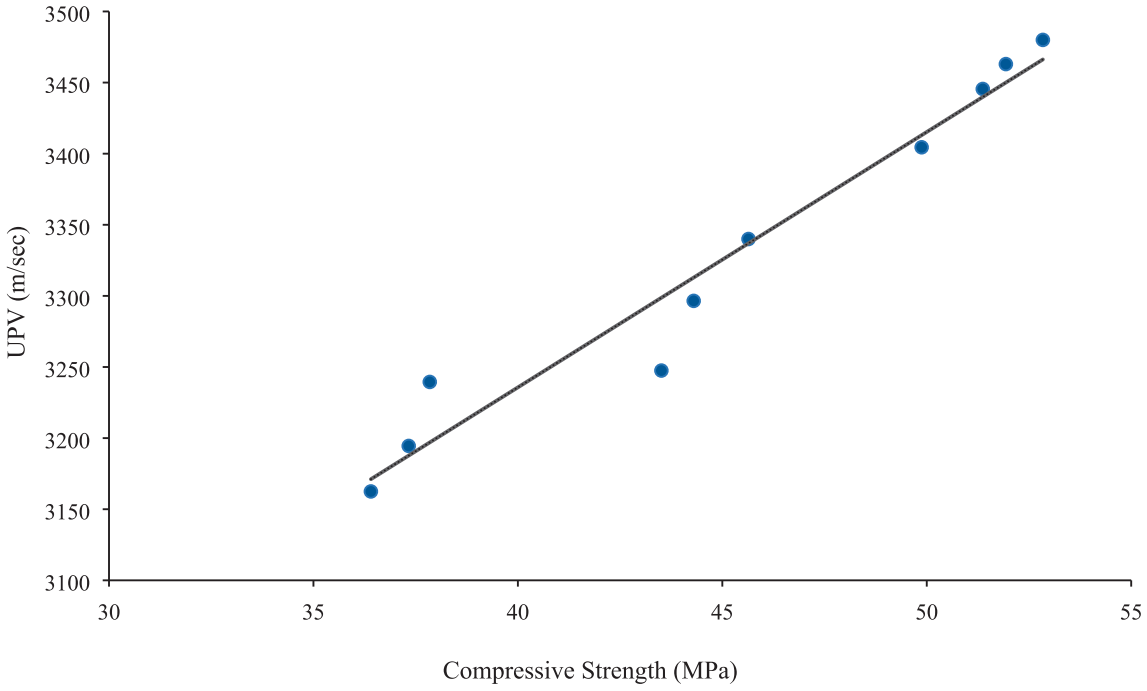

Fig. 4. The UPV-compressive strength relationship.

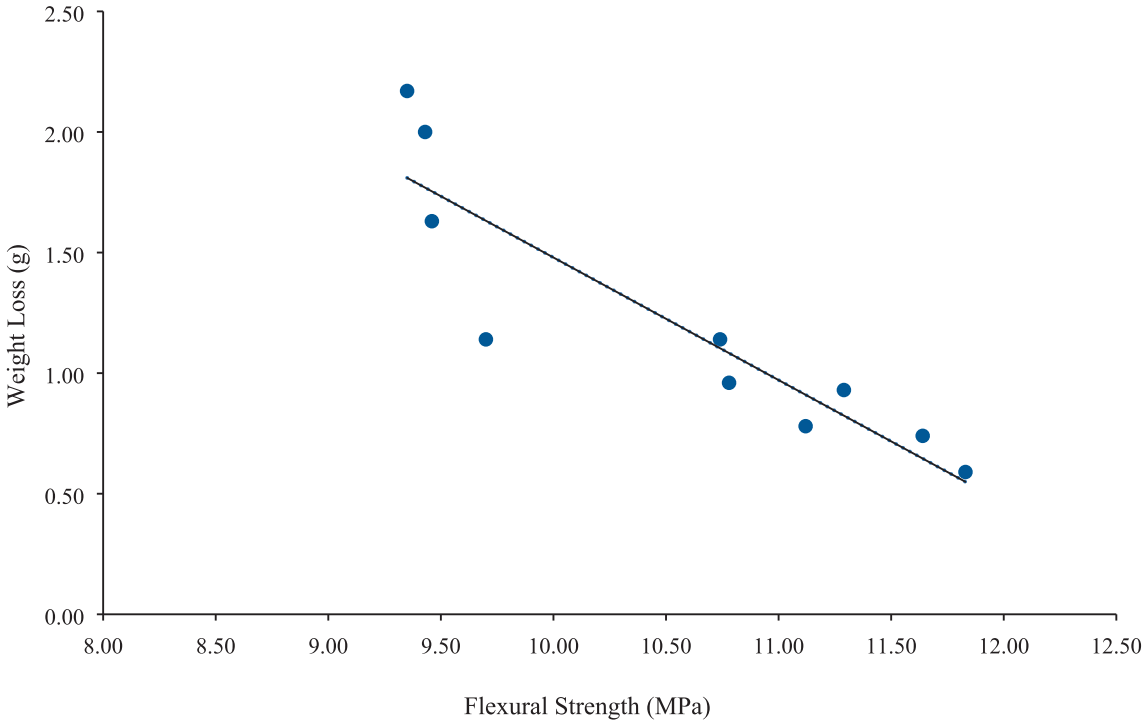

Fig. 5. The weight loss-flexural strength relationship.

increased grown age and fiber content indicated an improvement. Good bonding properties of basalt fibers with the geopolymer matrix lead to better structural performance along with high elastic modulus. The basalt fibers have good bonding properties with the geopolymeric matrix, so the reinforced geopolymers showed a better structural performance with higher elastic modulus. These findings were compared with the previous studies [14,35,66]. Natali et al. investigated the flexural strength of samples containing various fibers. All of the fibers showed a good performance in flexural strength [66].

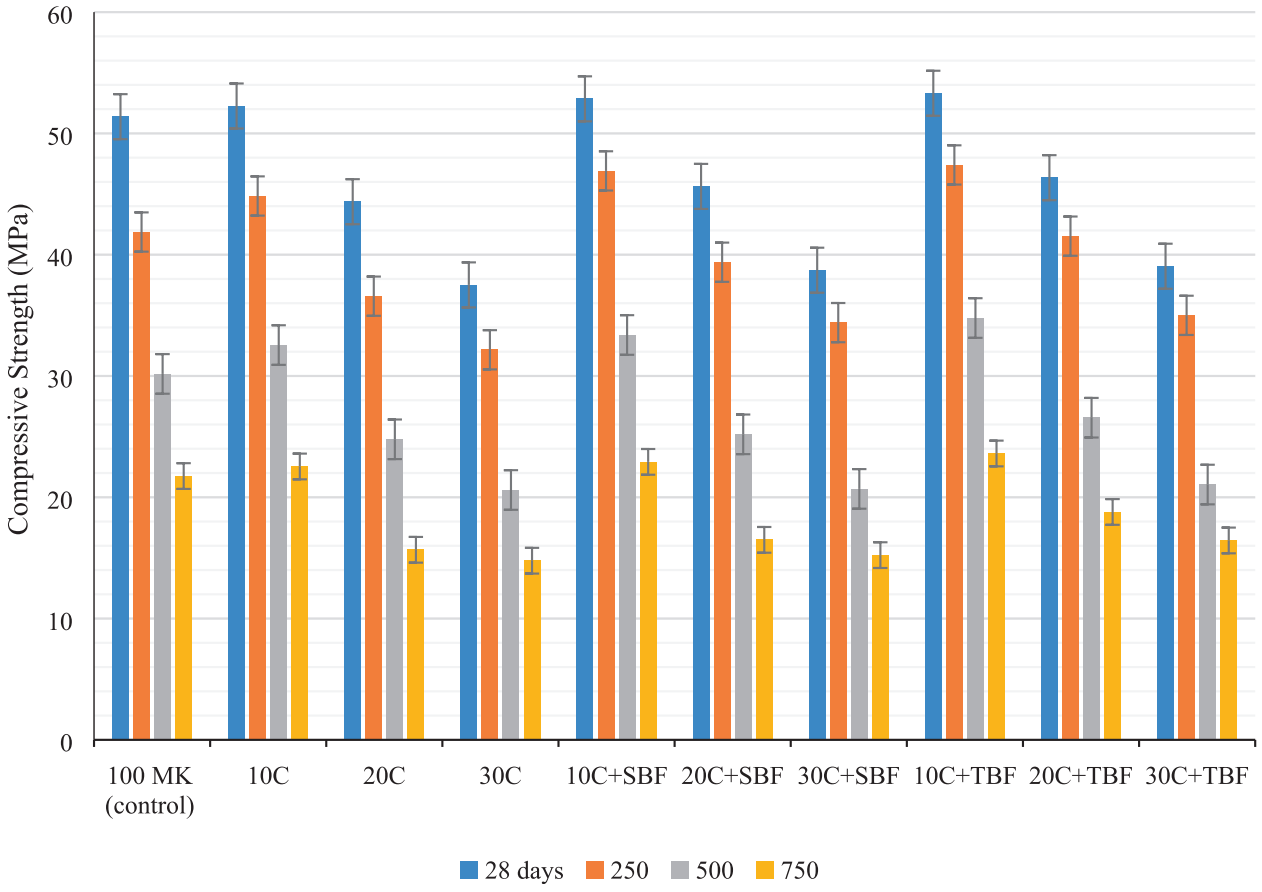

Fig. 6. Results of compressive strength after high-temperature effect.

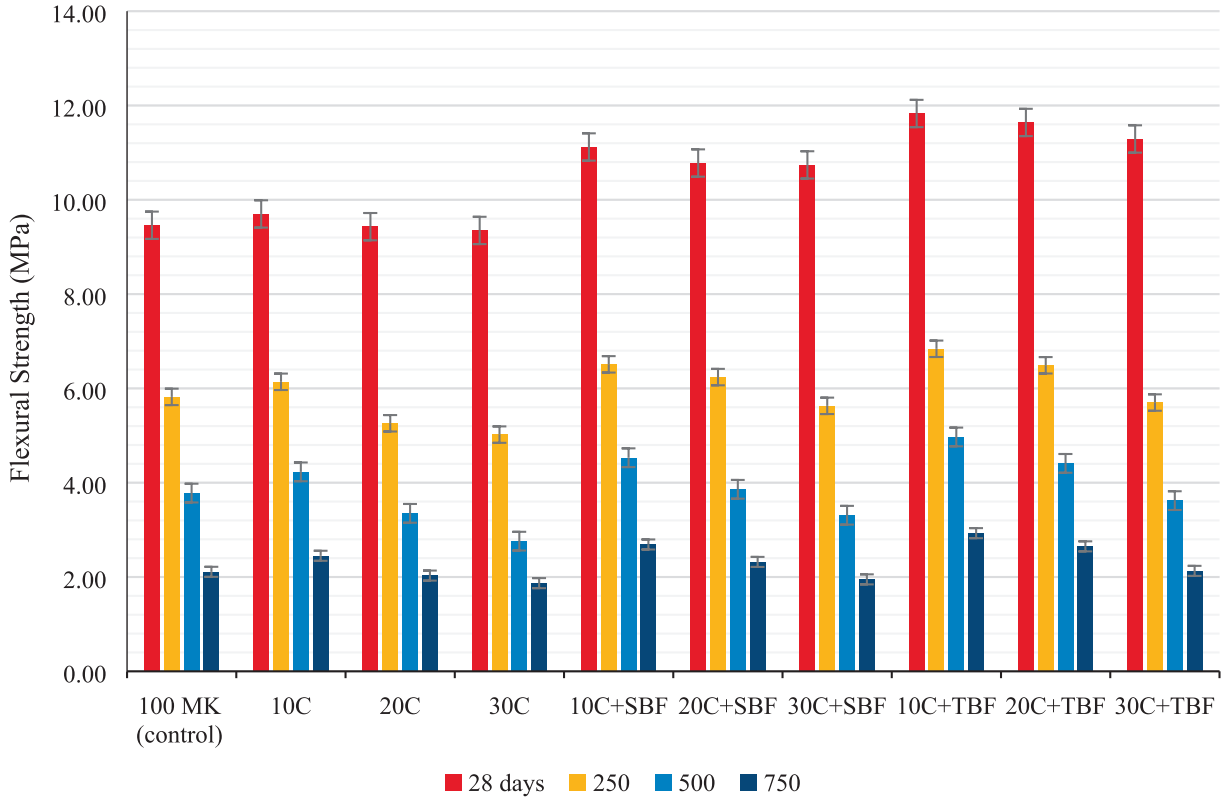

Fig. 7. Results of flexural strength after high-temperature effect.

Table 7
Losses in the compressive strength after elevated temperatures (%).

	250 °C	500 °C	750 °C
100 MK (control)	18.51	41.28	57.67
10C	14.20	37.72	56.87
20C	14.26	44.15	60.62
30C	17.56	45.08	64.28
10C + SBF	11.16	36.84	56.63
20C + SBF	11.34	44.80	60.67
30C + SBF	13.70	46.57	63.86
10C + TBF	10.40	34.76	55.71
20C + TBF	10.27	42.70	57.90
30C + TBF	11.09	46.09	59.46

Table 8
Losses in the flexural strength after elevated temperatures (%).

	250 °C	500 °C	750 °C
100 MK (control)	38.48	60.04	77.70
10C	36.70	56.39	76.74
20C	44.22	64.48	79.47
30C	46.31	70.58	83.00
10C + SBF	33.46	53.26	75.81
20C + SBF	42.12	64.19	78.48
30C + SBF	45.58	69.18	81.84
10C + TBF	32.18	51.99	75.23
20C + TBF	41.24	−62.11	77.29
30C + TBF	43.51	−67.94	81.12

Amuthakkannan et al. investigated the importance of fiber content and length on the engineering properties of composites. In their research, it was reported that the flexural strength increased importantly with the increment of fiber length and content [35]. Dias and Thaumaturgo investigated flexural behavior by using basalt fibers. Also, with every increase of fiber content, they showed an improvement in flexural behavior, and 1.0% basalt fiber enhanced the flexural strength by 23.80% according to fiberless samples. The flexural strength results after high temperature showed that all mixtures gained an important improvement compared to the control specimen. The basalt fiber specimens showed a better performance than the other samples with lower strength ratios.

The compressive strength reduction rates of colemanite-substituted fiberless samples were between 56.87% and 64.28% at 750 °C and between 56.63% and 63.86% for short basalt fiber samples and between 55.71% and 59.46% for long basalt fiber samples. Basalt fiber supplementation was similar to the results of 28 days and increased the results [47].

Flexural strength reduction rates of colemanite-substituted fiberless samples were between 76.74% and 83% at 750 °C and between 75.81% and 81.84% for short basalt fiber samples and between 75.23% and 81.12% for long basalt fiber samples. Flexural strength results increased with basalt fibers [47].

Colemanite substitution increased compressive strength results up to 10% but decreased results with more colemanite substitution. The compressive strength results of 10C, 20C and 30C samples at a temperature of 750 °C were 22.54 MPa, 15.67 MPa, and 14.77 MPa, respectively. The compressive strength results of 10C + SBF, 20C + SBF and 30C + SBF samples at a temperature of 750 °C were 22.92 MPa, 16.49 MPa, and 15.23 MPa, respectively. The compressive strength results of 10C + TBF, 20C + TBF and 30C + TBF samples at a temperature of 750 °C were 23.61 MPa, 18.79 MPa and 16.44 MPa, respectively.

The flexural strength results of 10C, 20C and 30C samples at a temperature of 750 °C were 2.45 MPa, 2.03 MPa, and 1.87 MPa, respectively. The flexural strength results of 10C + SBF, 20C + SBF and 30C + SBF samples at a temperature of 750 °C were 2.69 MPa, 2.32 MPa, and 1.95 MPa, respectively. The flexural strength results of 10C + TBF, 20C + TBF and 30C + TBF samples at a temperature of 750 °C were 2.93 MPa, 2.65 MPa and 2.13 MPa, respectively.

3.6.2. Ultrasonic pulse velocity results

With the elevated temperatures, the sample pore structure growth and the water evaporation in the matrices increase. Additional voids occur with the loss of mass. Additional voids are the cause of the fall in the UPV results [67]. The UPV results are shown in Fig. 8 and the reduction ratios are given in Table 9. The UPV results after elevated temperatures indicate that the reinforced specimens with basalt fiber performed slightly better according to other samples. All samples showed similar behavior and remarkable changes with UPV values after 250 °C and thereupon a large drop. Geopolymer samples indicated a dramatic decrease after 250 °C for the UPV results. This situation shows that the geopolymeric matrix has been severely damaged after exposure to 250 °C and is also in agreement with the strength loss. Due to the larger cracks formation after the elevated temperatures and the fibers' melting process over 250 °C in the geopolymeric matrix, the ultrasonic velocity waves' propagation time was delayed and lower values were obtained.

The UPV reduction rates of colemanite-substituted fiberless samples were between 70.72% and 73.09% at 750 °C and between 69.35% and 71.49% for short basalt fiber samples and between 68.25% and 70.84% for long basalt fiber samples. Basalt fiber supplementation was similar to the results of 28 days and increased the results [47]. Colemanite substitution increased ultrasonic pulse velocity results up to 10% but decreased results with more colemanite substitution. The UPV results of 10C, 20C and 30C samples at a temperature of 750 °C were 1017 m/s, 923 m/s and 856 m/s, respectively. The ultrasonic pulse velocity results of 10C + SBF, 20C + SBF and 30C + SBF samples at a temperature of 750 °C were 1072 m/s, 989 m/s and 914 m/s, respectively. The ultrasonic pulse velocity results of 10C + TBF, 20C + TBF and 30C + TBF samples at a temperature of 750 °C were 1115 m/s, 1003 m/s and 949 m/s, respectively.

3.6.3. Results of weight loss

Weight-loss rates with temperature increase are shown in Fig. 9. When the weight-loss results were examined, smaller weight loss was observed for other samples according to the control sample. So the fibers perform significant progress in weight loss reduction. Furthermore, it has been shown that the increase in fiber length positively affects the performance of geopolymer mortars after elevated temperatures. Also, colemanite substitution reduced weight loss. After elevated temperatures, a dehydration reaction occurs in the matrice and the present moisture moves towards the sample's surface and goes away. Due to this condition, internal damage occurs in the microstructure and leads to weight loss increases. The major reason for the loss before 600 °C was the evaporation of condensed hydroxyl groups along with free water. Above 600 °C, weight loss increase because of the fiber and matrix interfacial reactions was observed. Increasing was seen in weight loss because of the significant fiber degradation. Nevertheless, with the fiber, the weight loss decreased according to the control sample [68]. So, the geopolymer specimens showed

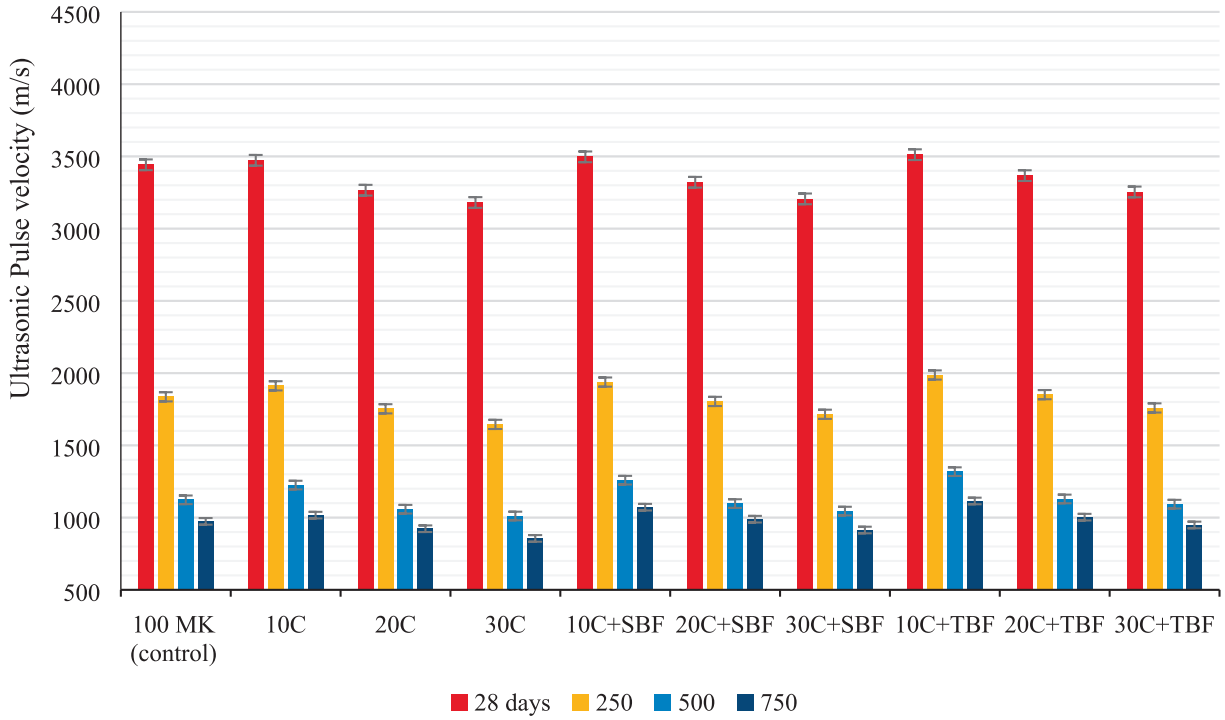

Fig. 8. Results of ultrasonic pulse velocity after high-temperature effect.

Table 9
Losses in the UPV after elevated temperatures (%).

	250 °C	500 °C	750 °C
100 MK (control)	46.66	67.37	71.70
10C	44.95	64.73	70.72
20C	46.33	67.61	71.74
30C	48.29	68.22	73.09
10C + SBF	44.58	64.00	69.35
20C + SBF	45.68	66.97	70.22
30C + SBF	46.51	67.40	71.49
10C + TBF	43.42	62.47	68.25
20C + TBF	45.03	66.47	70.21
30C + TBF	45.94	66.41	70.84

decreased engineering properties and fractures in a very brittle manner [69].

Weight-loss rates in colemanite-added fiberless samples were between 1.02% and 1.34% at 250 °C, between 2.37% and 2.72% at 500 °C and between 4.23% and 4.68% at 750 °C. The weight-loss rates for colemanite-added short basalt fiber specimens were between 0.93% and 1.23% at 250 °C, between 2.22% and 2.62% at 500 °C, and between 4.12% and 4.48% at 750 °C. Also, the weight-loss rates in colemanite-added long basalt fiber specimens were between 0.72% and 1.01% at 250 °C, between 1.99% and 2.38% at 500 °C and between 3.87% and 4.15% at 750 °C.

3.6.4. Visual inspection and analyses

Visual examination of samples exposed to 750 °C temperature was performed immediately after the test (Figs. 10 and 11). By examining samples exposed to high temperature, a color change was noticed [47]. However, the cracks on the surfaces were small and the samples protected their stable condition. With this situation, the effect of temperature after 750 °C becomes more pronounced. The samples' surface tends to be coarser. At 750 °C, tiny cracks that are become more apparent and a brittle structure is formed. The major reason is the destruction of the main chains of the geopolymeric system.

The SEM analysis images after the temperature effect of 250 and 500 °C are given in Figs. 12 and 13. After the temperature effect of 250 °C, it was understood that there were no significant cracks in microstructures. After the temperature effect of 500 °C, the increase in cracks was noticed [70]. Concerning the samples' micrographs after exposure to heat effect, the geopolymeric network's viscous sintering occurs and shows the main conclusion of the ensuing thermal shrinkage because of elevated temperatures [71]. This situation happens to more significant after the elevated temperatures so it ensues in fewer pores which causes the geopolymer specimens to collapse. But it was understood that geopolymer samples continued to maintain its structure. 10C + TBF sample also showed the continuity of the matrix formed and a good bonding during the geopolymerization.

Figs. 14 and 15 show the FT-IR spectra of the 10C + TBF sample before and after the 500 °C temperature. 997.54 and 980.95 cm^{-1} respectively indicate the previous and subsequent wavelengths of the 10C + TBF sample. These numbers indicate the Si–O–Al bonds corresponding to the asymmetric stretching vibrations. Si–O–Al bonds showed a decrease according to the pre-experiment but the sample was found to protect Si–O–Al bonds. Also, the intensity of the bands before the experiment was found to be in the range of about 3600 and 1450 cm^{-1} [72,73].

The DTA and TGA curves are shown in Fig. 16 for the 10C + TBF sample. The red curves here correspond to weight loss. In the 10C + TBF sample, 5.878% weight loss was found in the TGA analysis after 500 °C. As can be seen, it was found that geopolymer composite samples retained their stability after a temperature

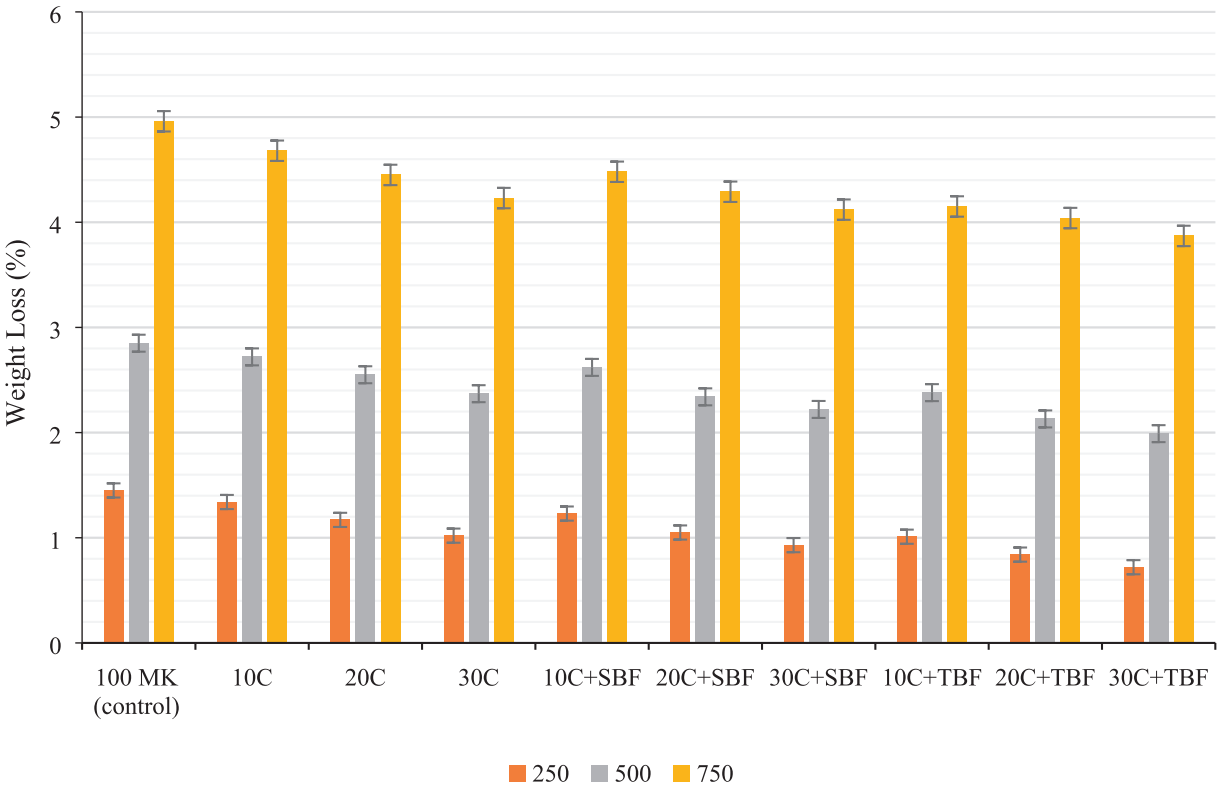

Fig. 9. Results of weight-loss rates after high-temperature effect.

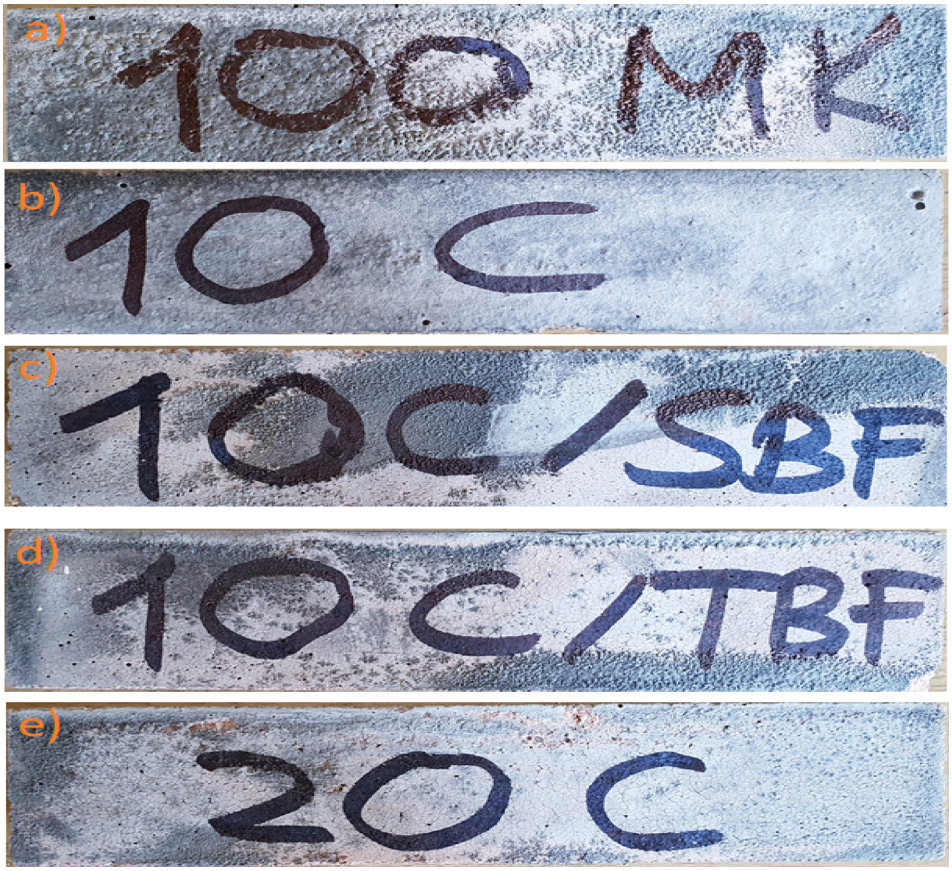

Fig. 10. a) 100MK, b) 10C, c) 10C + SBF, d) 10C + TBF, e) 20C samples after high temperature.

Fig. 11. a) 20C + SBF, b) 20C + SBF, c) 30C, d) 30C + SBF, e) 30C + TBF samples after high temperature.

effect of 500 °C. The weight loss is mostly in the range of 0–380 °C because of the evaporation of bound and free water present in the matrix. The endothermic peaks occurring in this range were observed in DTA curves. After 700 °C, the weight loss became constant. In this case, it is because of the chemically bound water and hydroxyl groups (OH) evaporation in the geopolymer [74,75].

The main structure of classical geopolymers was protected and showed lower microstructural deterioration and less strength loss after higher temperatures according to the XRD analysis [47,76]. Fig. 17 shows the XRD spectra of the 10C + TBF sample after high temperatures of 500 °C. For 10C + TBF sample at 600 °C, amorphous hump covering quartz peaks at 28° in the 10C + TBF sample was preserved, showing that these phases were inert along with the elevated temperatures [76].

3.7. Sulfuric acid effect test

Geopolymer mortar samples were exposed to 10% Hydrosulfuric Acid (H_2SO_4) for 3 months after 28 days. Strength results of 1, 2 and 3 months were compared with the 28 days' results. Also, the UPV results with the solution effect were compared with the 28-day results (Figs. 18–20). As a result of the test, the samples were taken out from the solutions and left to dry at room conditions. After drying, the surfaces of the samples were cleaned with the wire brush and the weight losses of the samples were determined (Fig. 21). The maximum deterioration in all samples was observed in 3 months. The major reason for the decrease in strength is the deterioration of the alumina-silicate bonds due to the effect of sulfuric acid. Also, the zeolites' formation and geopolymer products' depolymerization increases the loss of strength. But the geopolymer mechanism, which fabricates polymerization reaction products with strong alumina-silicate bonds, is not handily influenced by acid exposure [77].

Geopolymer samples have better resistance to chemical effects than Portland-based samples. The stability of geopolymer samples formed in the acidic environment is related to the crystal phase formation in the aluminosilicate structure, the more crystalline phase formation in the aggressive environment increases the stability. Also, the morphological structure is the other cause of resistance to acid activity and low Ca content plays a role in providing superior endurance. The final products resulting from the acid attack are the calcium salt and also the hydrogels of aluminum, silicon and iron oxides. The low calcium rate reduces the formation of synthetic products that affect durability [77].

In the 10C samples, 40.25 MPa, 34.40 MPa, and 26.62 MPa were obtained respectively in 1, 2 and 3 months, whereas the strength results were increased with the basalt fiber effect and the results of 10C + SBF were 42.33 MPa, 36.18 MPa and 27.72 MPa in three months, respectively. The results of 10C + TBF were 43.69 MPa, 37.64 MPa and 29.16 MPa for three months, respectively. Amuthakkannan et al. investigated the fiber content and length of the strength properties of geopolymer composites. In their research, it was reported that the flexural strength increased importance as the fiber length and content increased [35]. Colemanite waste has improved results if it is used as substitution by 10%.

The reduction in the flexural strength under the influence of acid is due to reasons similar to the compressive strength [77]. In the 10C samples, the residual flexural strengths were found respectively as 7.1 MPa, 5.98 MPa and 4.87 MPa in 1, 2 and 3 months, whereas the strength results were increased with the basalt fiber effect and 8.45 MPa, 6.73 MPa and 5.52 in three months respectively in the 10C + SBF samples. In the 10C + TBF samples,

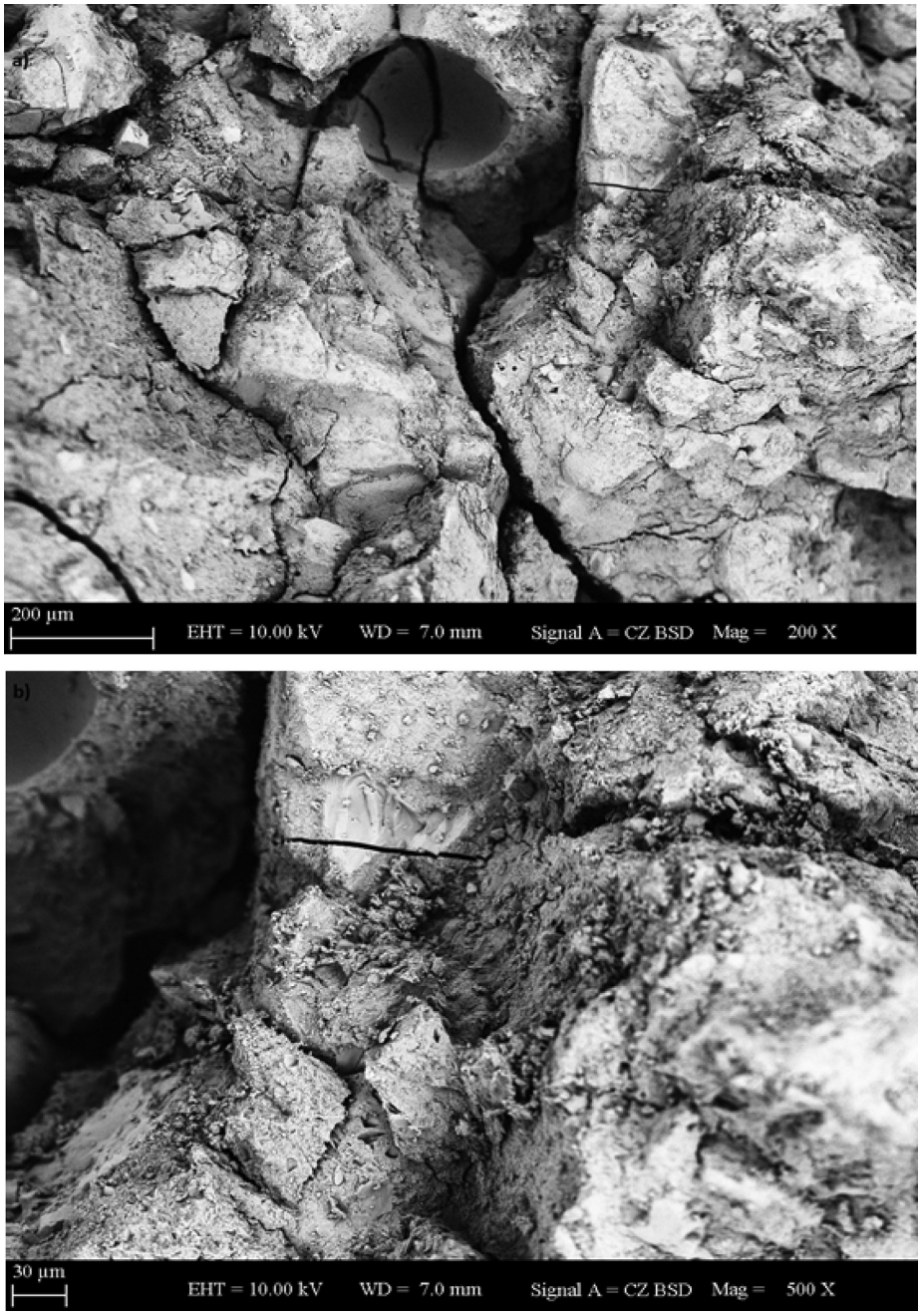

Fig. 12. SEM micrographs for 10C + TBF sample after 250 °C.

8.86 MPa, 7.12 MPa and 5.83 MPa results were obtained in three months respectively.

The reduction in the UPV rates with the acid effect is due to the increase of microcracks in case of high exposure of the samples to sulfuric acid [77]. If the voids ratio increase, the waves' transition time will increase and the results will decrease. In the 10C samples, the ultrasonic pulse velocity were obtained respectively as 3129 m/s, 2878 m/s and 2446 m/s in 1, 2 and 3 months, whereas the results were increased with the effect of basalt fiber and 3105 m/s, 2926 m/s ve 2560 m/s in three months respectively in the 10C + SBF samples. In the 10C + TBF samples, 3165 m/s, 2949 m/s ve 2591 m/s results were obtained in three months respectively.

Weight loss due to sulfuric acid was low in 3 months. The major reason is the stability of the aluminosilicate structure present in the geopolymer sample. In the 10C samples, weight loss results were obtained as 0.36%, 0.73%, and 1.3% respectively in 1, 2 and 3 months, while the results were decreased with the effect of basalt fiber and 0.25%, 0.64% and 1.14% in 3 months respectively in the 10C + SBF samples. In the 10C + TBF samples, weight loss results were obtained as 0.19%, 0.57% and 0.92%, respectively.

After the sulfuric acid effect, some deterioration was observed on the sample surface. The damage was parallel to the high acid solution concentration. At the end of the experiment, the surface became softer, but not easily scratched. However, it was found that the samples were stable (Figs. 22 and 23).

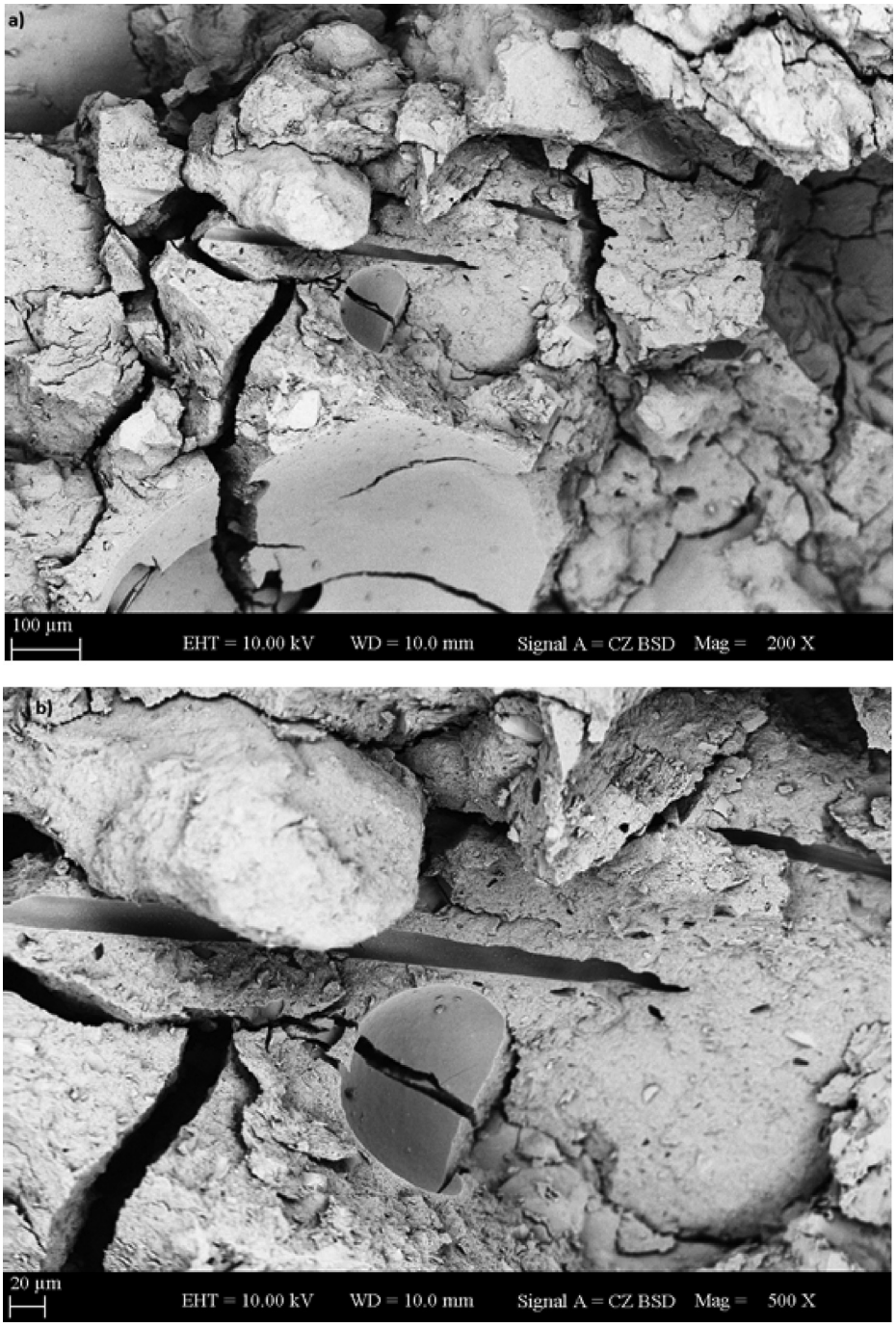

Fig. 13. SEM micrographs for 10C + TBF sample after 500 °C.

Microstructural changes in the 10C + TBF specimens after sulfuric acid effect at the end of 3 months are shown in Fig. 24. The geopolymer samples' microstructure after the acid effect was porous by the formation of microcracks resulting from the degradation of Si–O–Al bonds in the geopolymer gel. The reason for the cracks' formation is the shrinkage of the gel layer and due to this situation, the sulfuric acid is more easily transferred to the internal microstructural areas. The observed needle-shaped particles began to disappear by dissolving in the acid.

Analysis of XRD analysis after the effect of sulfuric acid showed that metakaolin-based geopolymer composites retained the basic structure [78]. Fig. 25 shows the XRD spectra of the 10C + TBF sample exposed to 10% sulfuric acid for 3 months. Significant changes were observed in the spectra after the acid effect. The peak intensities for the zeolite phases were decreased compared to the pretest levels. The quartz peaks corresponding to the typical amorphous geopolymer gel phase at 2θ between 27° and 28° were protected after exposure to the acid solution [79].

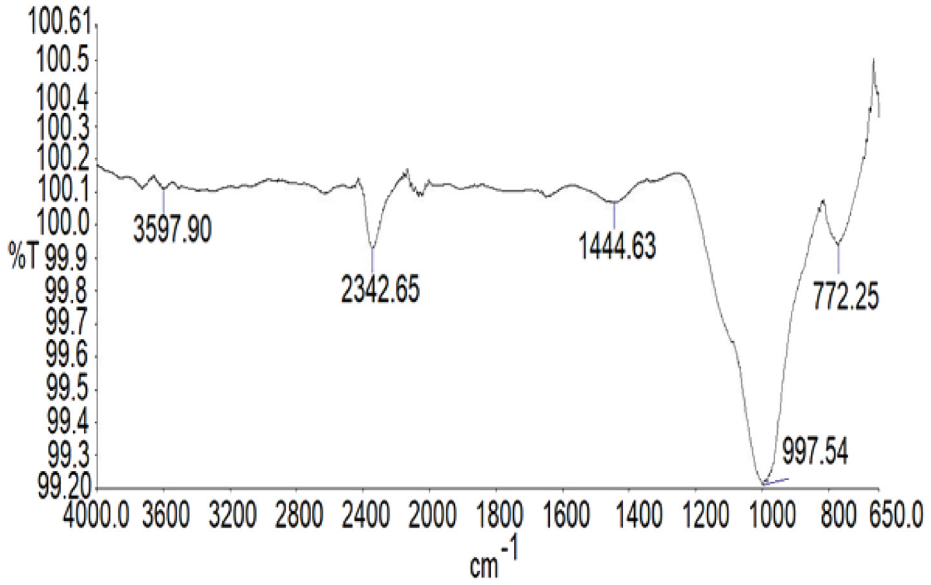

Fig. 14. FT-IR results of 10C + TBF sample before 500 °C.

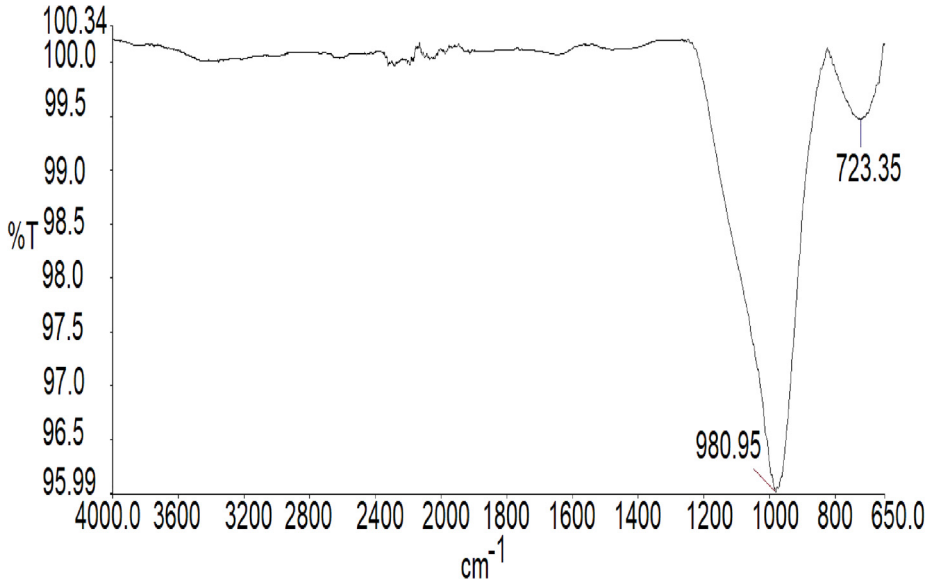

Fig. 15. FT-IR results of 10C + TBF sample after 500 °C.

Fig. 26 shows the FT-IR spectra of the 10C + TBF sample after the sulfuric acid effect. 984.05 cm^{-1} shows the wavelength after the experiment. This number indicates the Si–O–Al bonds corresponding to the asymmetric stretching vibrations. Si–O–Al bonds showed a limited decrease compared to the pre-experiment situation. Also, the intensity of the bands after the experiment was found to be between about 3050 and 1300 cm^{-1} [72,73].

The DTA and TGA curves are shown in Fig. 27 for the 10C + TBF sample. The red curves here correspond to weight loss. In the 10C + TBF sample, 0.732% weight loss was observed in the TGA analysis after the sulfuric acid effect. As can be seen, it was found that geopolymer composite samples retained their stability after the sulfuric acid effect. The weight loss was very small and mostly in the range of 0–300 °C because of the evaporation of bound and free water present in the matrix. The endothermic peaks occurring in this range were observed in DTA curves. After 700 °C, the weight loss became constant. In this case, it is because of the chemically bound water and hydroxyl groups (OH) evaporation in the geopolymer [74,75].

3.8. Freezing-thawing test

The results of the 90 cycles test were compared with the 28th day. The samples' UPV, residual strengths, and weight loss

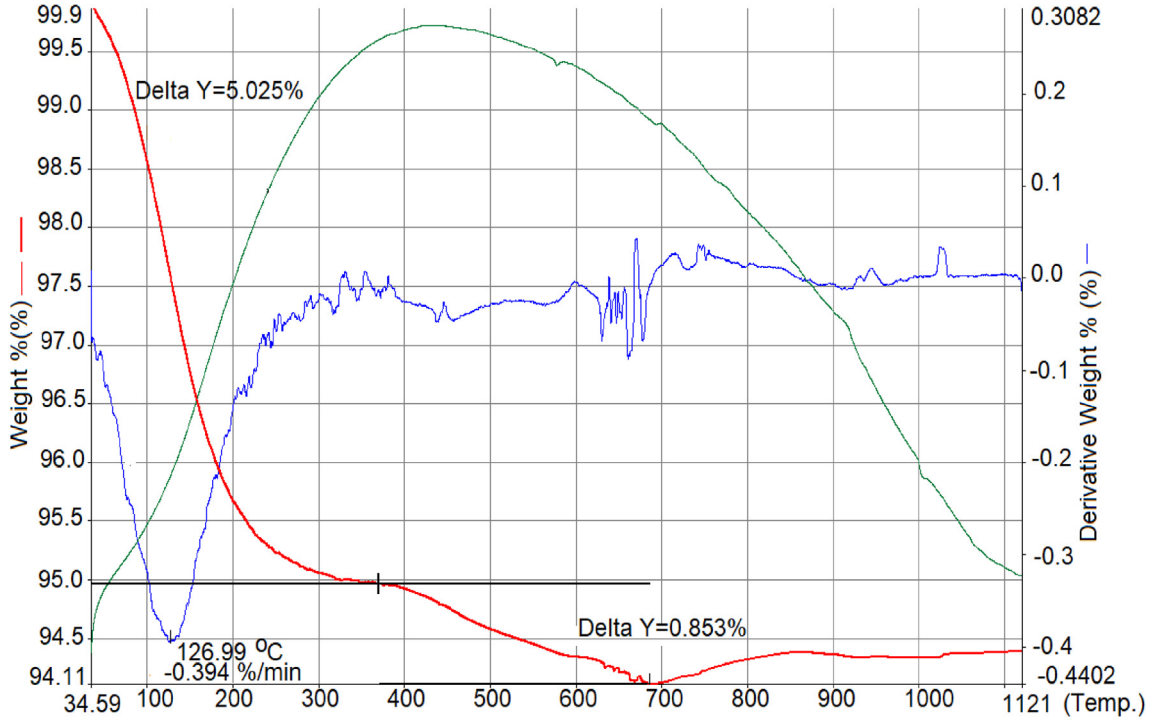

Fig. 16. TGA-DTA results of 10C + TBF sample after 500 °C.

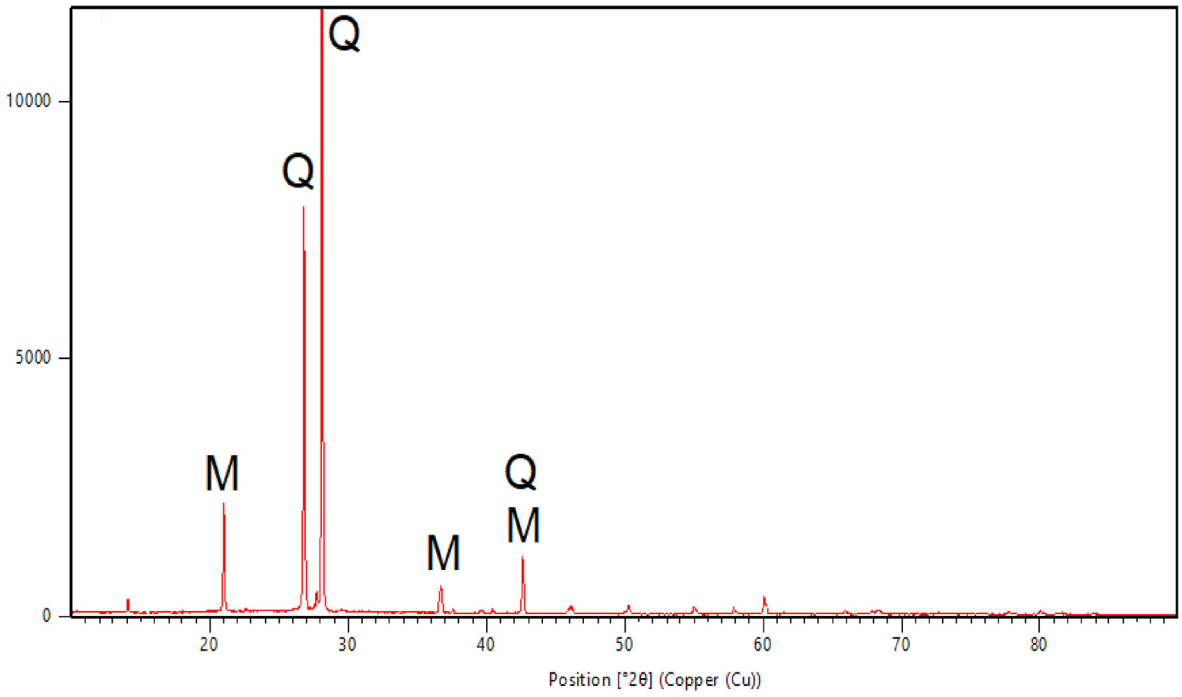

Fig. 17. XRD patterns of 10C + TBF sample after 500 °C.

results were given in Figs. 28–31. The geopolymeric matrix's compact structure creates a good adhesion level. So geopolymer composites showed good performances after freezing-thawing. After 90 cycles, the losses in the strength and UPV results were low. When using basalt fiber, the UPV and strength losses decreased and the results were higher. The behavior in the using fibers was like the condition before the test. The weight losses were very small due to the humidity of the test environment. The results of the test were consistent with the previous studies [74,75].

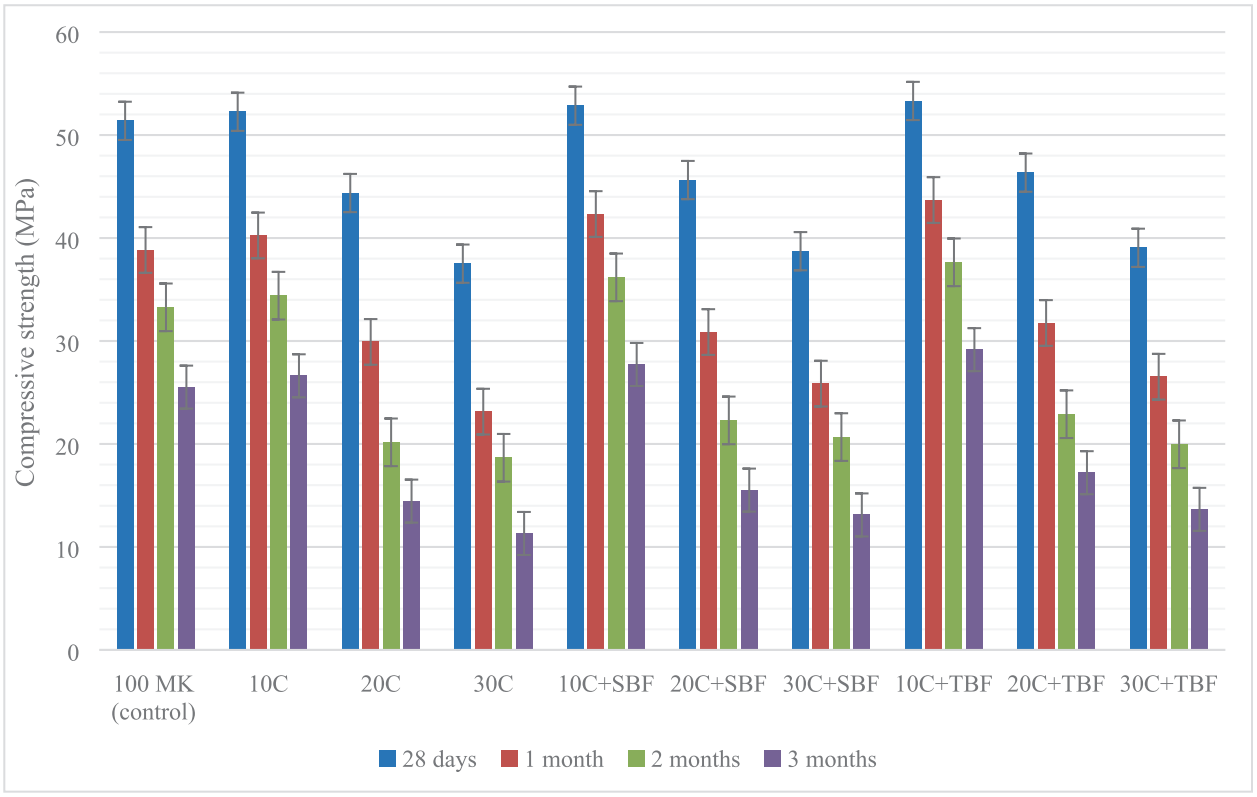

Fig. 18. Residual compressive strengths after exposure to sulfuric acid.

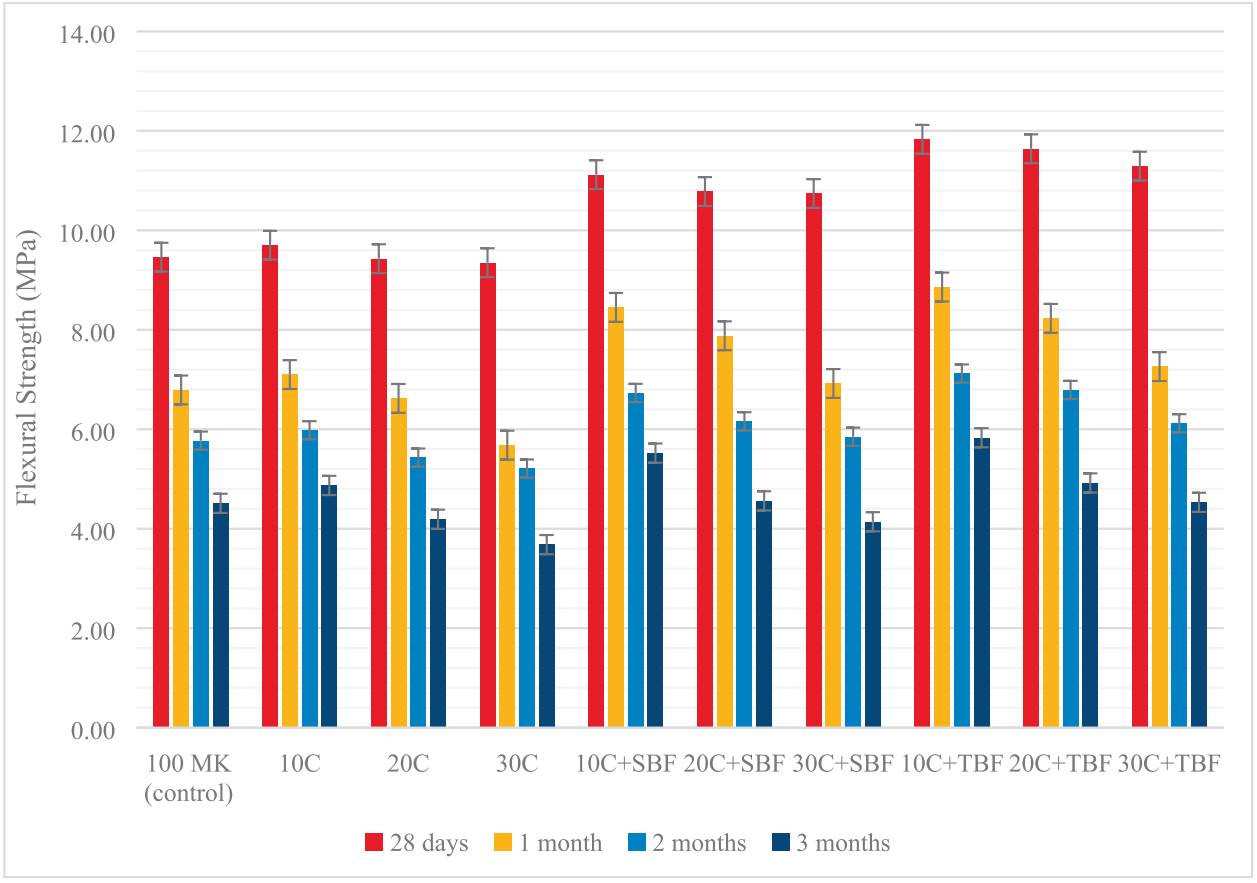

Fig. 19. Residual flexural strengths after exposure to sulfuric acid.

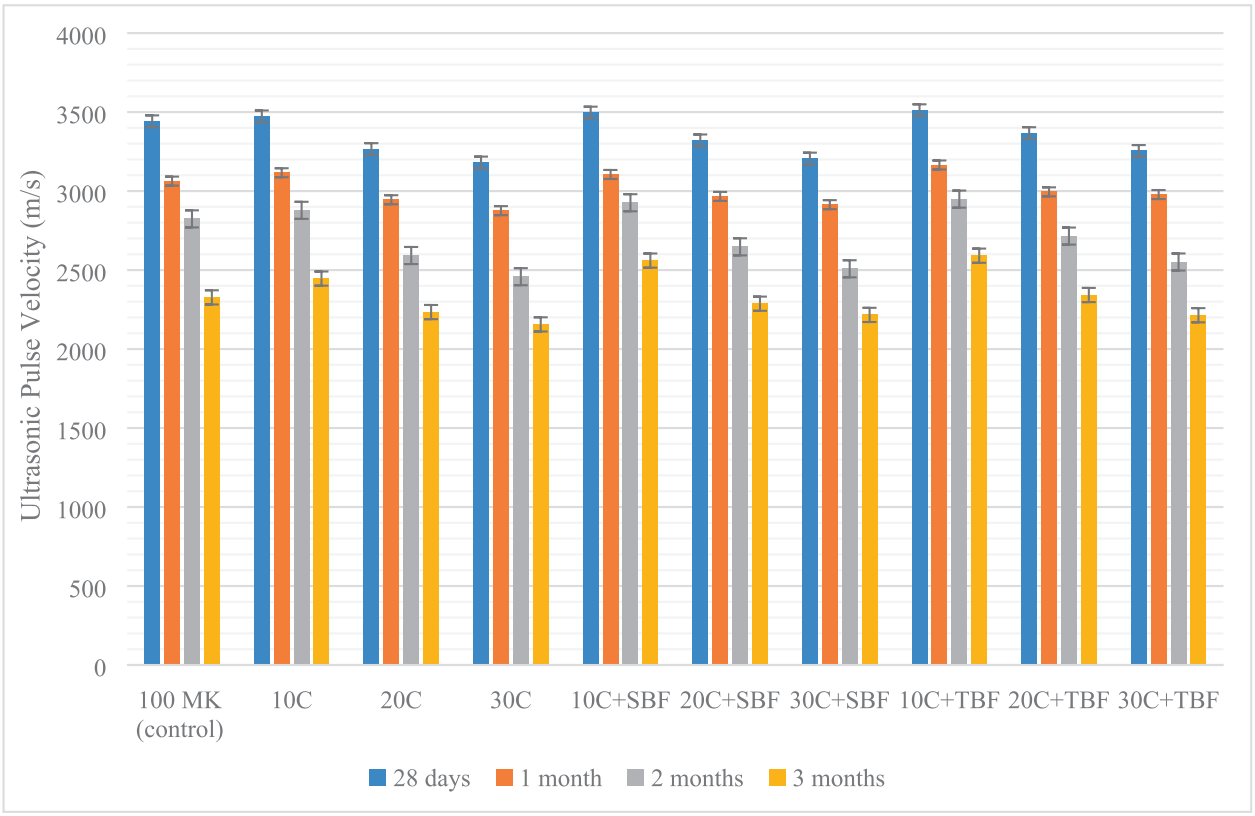

Fig. 20. Ultrasonic pulse velocity results after exposure to sulfuric acid.

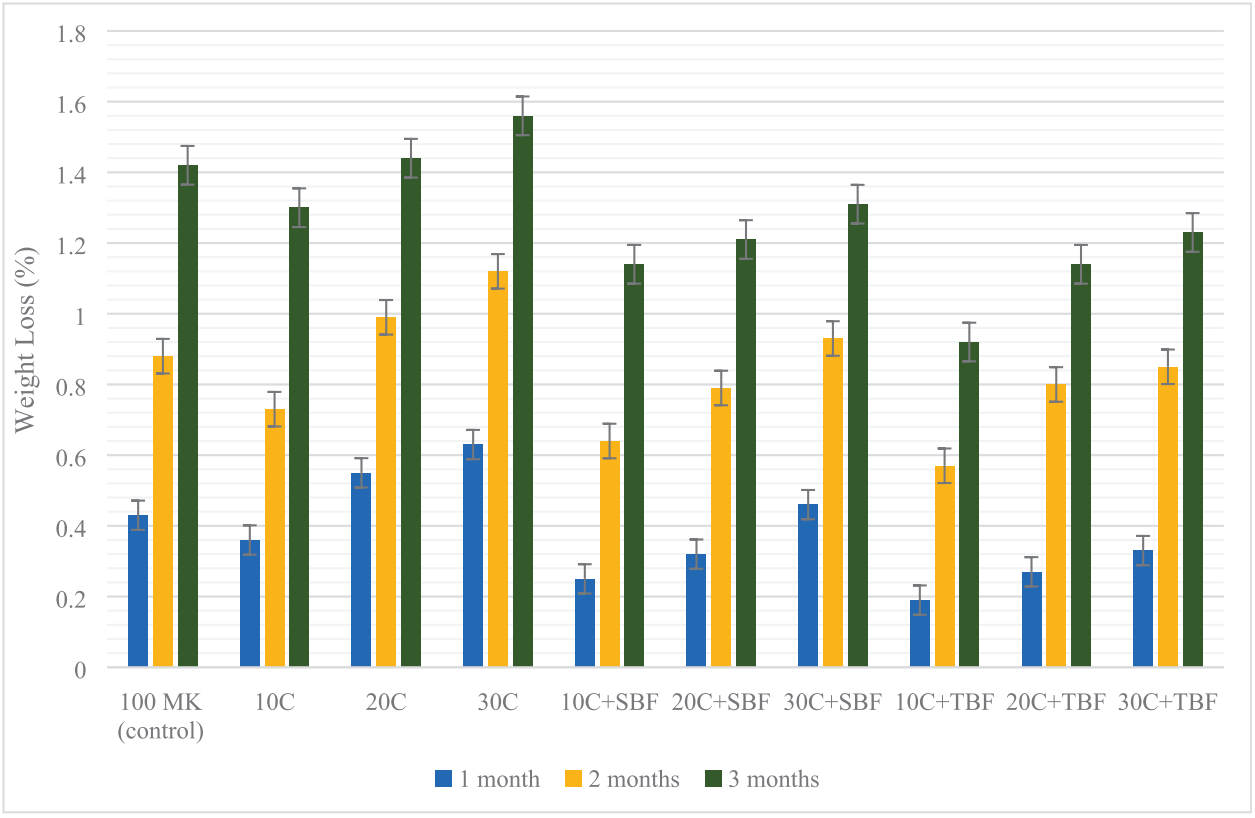

Fig. 21. Weight loss results after exposure to sulfuric acid.

Fig. 22. Visual inspection after exposure to sulfuric acid over 3 months.

After the test, the highest result for compressive strength was obtained with 38.53 MPa and in the 10C + TBF sample, while the lowest result was 19.52 MPa in the 30C sample. The highest residual flexural strength result was obtained with 9.56 MPa and in the 10C + TBF sample while the lowest result was 5.85 MPa in the 30C sample. When the ultrasonic pulse velocity results were examined, the highest and lowest values after the test were 3409 m/s and 2948 m/s. The lowest result was obtained with 0.43% and in the 10C + TBF sample as weight loss, while the highest result was 0.87% in the 20C sample. Visual inspection for the samples was performed at the end of the test and given in Fig. 32. While there was no significant change in the samples' external appearance, the main event that affects the deterioration is the water expansion in the permeable structure. Freezing allows water to expand to 9% by volume, which creates a hydraulic pressure [80].

The air spaces in the specimen supply an area where ice could expand. Nonetheless, after the useable free space is filled up, the freezing ice produces pressure on the cement matrix round it. After the strength result passes over concrete's stress, micro-cracks and deterioration happen [81,82]. Since the first geopolymer's strength is superior, it can withstand higher pressures than freezing water afore micro-cracks happen.

Microstructural studies showed that micro-cracks appear in the interface between aggregate and paste because of capillary water expansion during freeze-thaw cycles. These micro-cracks can result in the mortar to deteriorate. Crystals happen after exposure to freeze-thaw cycles. This is expected to reduce strength [83]. For all samples, weight loss after the 90 cycles was less than 1%.

The microstructural analysis examined in the 10C + TBF sample after 90 cycles are shown in Fig. 33. Post-test SEM images of geopolymer samples showed micro cracks. This explains the strength and loss of ultrasonic pulse velocity. In spite of this, it was observed that the geopolymer sample retained its stability. When the XRD analysis was performed in the 10C + TBF sample, in the same way, it was observed that Quartz peaks were between 22° and 28° while the peaks were not changed according to the pre-test conditions (Fig. 34).

Fig. 35 shows the FT-IR spectra of the 10C + TBF sample after the freezing-thawing test. 987.22 cm^{-1} shows the wavelength after the experiment. This number indicates the Si –O– Al bonds corresponding to the asymmetric stretching vibrations. The change in Si–O–Al bonds after the test was limited compared to the first case. Also, the intensity of the bands after the experiment was found to be between about 3050 and 1315 cm^{-1} [72,73].

The DTA and TGA curves are shown in Fig. 36 for the 10C + TBF sample. The red curves here correspond to weight loss. In the 10C + TBF sample, 0.619% weight loss was observed in the TGA analysis after the freezing-thawing test. As can be seen, it was found that geopolymer composite samples retained their stability after the freezing-thawing test. The weight loss was very small

Fig. 23. Visual inspection after exposure to sulfuric acid over 3 months.

and mostly in the range of 0–300 °C because of the chemically bound water and hydroxyl groups (OH) evaporation in the matrix. Endothermic peaks occurring in this range were observed in DTA curves [74,75].

4. Conclusions

For this paper, engineering properties were investigated in the case of colemanite substitution with basalt fiber reinforced geopolymer composites prepared using metakaolin as the major binder material:

- According to the results, colemanite substitution yielded an improvement regarding strength properties and ultrasonic pulse velocity test results by up to 10% and decreased at higher rates.
- The compressive strength results showed that basalt fibers with a length of 24 mm had better results than basalt fibers with a length of 12 mm. This can be attributed to the effect that holding mortar particles more robustly is possible with a longer anchoring. At the same time, the longer basalt fiber has a significant and positive effect on the flexural strength of the mortar sample.
- Geopolymer specimens showed a significant reduction in strength results due to dehydration and water evaporation with thermal reactions after 500 °C. When the reduction rates of the flexural strength results were examined, it was determined that they were higher compared to compressive strength. The cause of this situation is the formation of imperfections such as the growth of porous structures and the spreading of cracks along with the temperature.
- With the increase in temperature, the sample pore structure's growth and the water evaporation in the matrices increase. Additional voids occur with the loss of mass. Additional voids are the cause of the fall in the UPV results. Colemanite substitution reduced weight loss after the high-temperatures. Dehydration and moisture loss in samples produced under elevated temperatures lead to weight loss and microstructure damage.
- Geopolymer samples have better resistance to sulfuric acid effect. The stability of geopolymer samples formed in the acidic environment is related to the crystal phase formation in the aluminosilicate structure, the more crystalline phase formation in the aggressive environment increases the stability. With using basalt fiber, the UPV and strength losses decreased and the results were higher.
- The geopolymeric matrix's compact structure creates a good level of adhesion. Due to this situation, geopolymer composites showed good performances after freezing-thawing. After 90 cycles, the losses in the strength and UPV results were low.

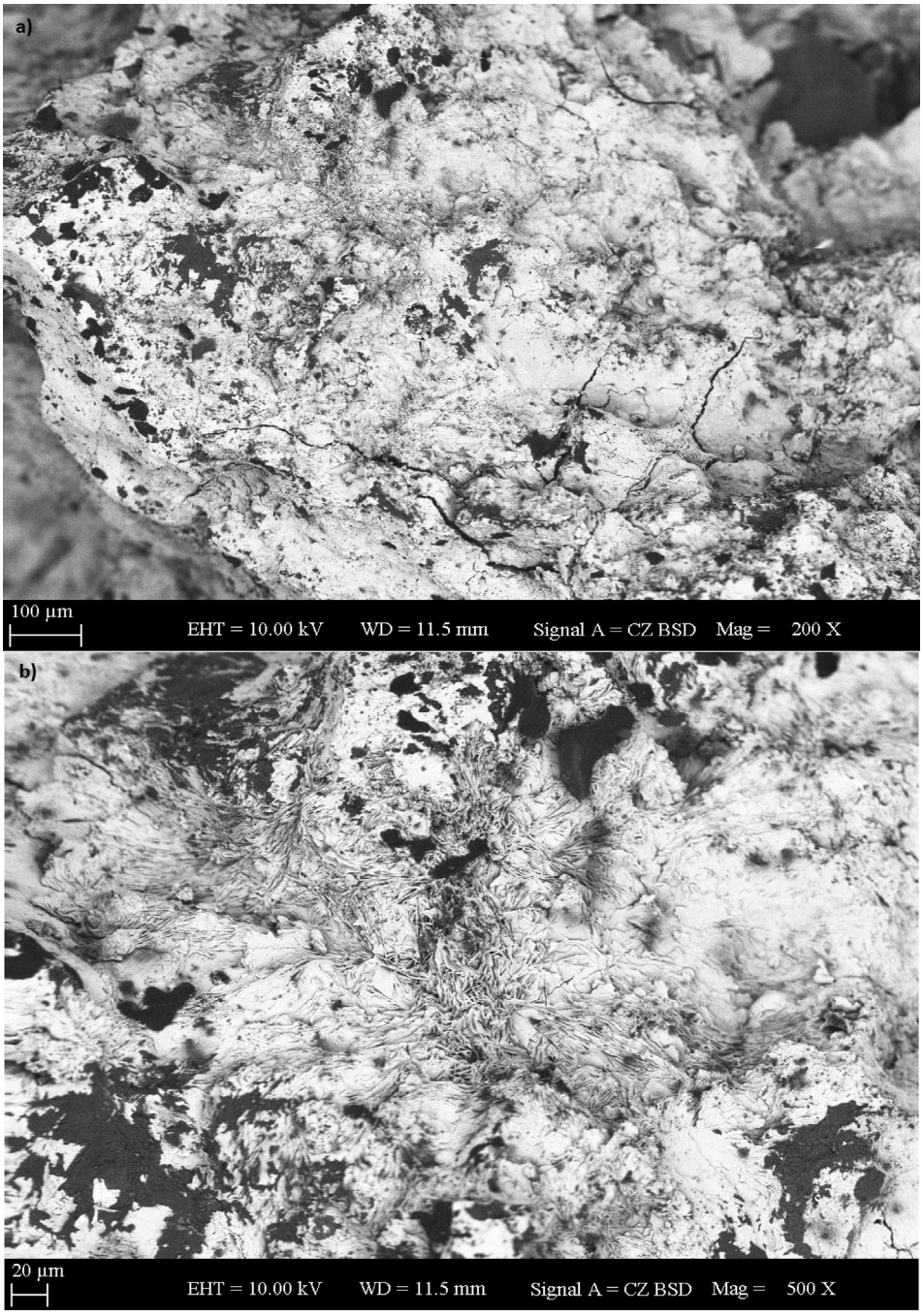

Fig. 24. SEM micrographs of 10C + TBF after exposure to sulfuric acid over 3 months.

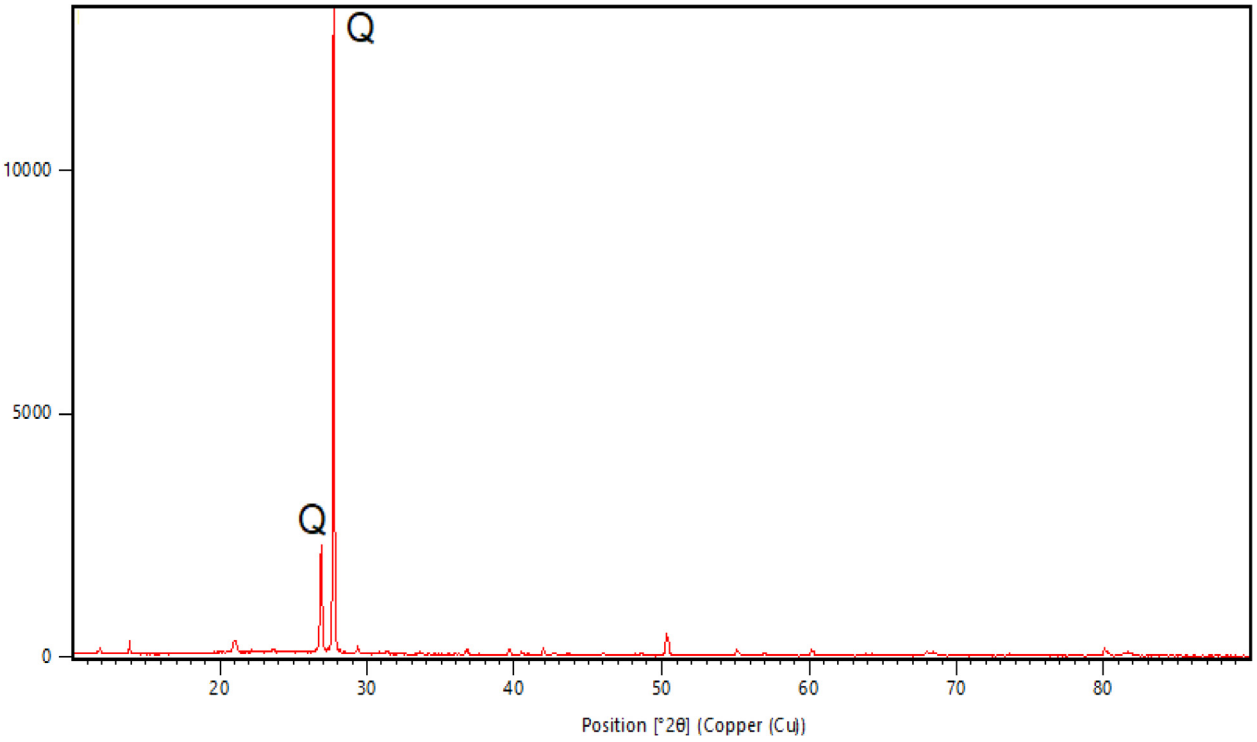

Fig. 25. XRD patterns of 10C + TBF sample after exposure to sulfuric acid over 3 months.

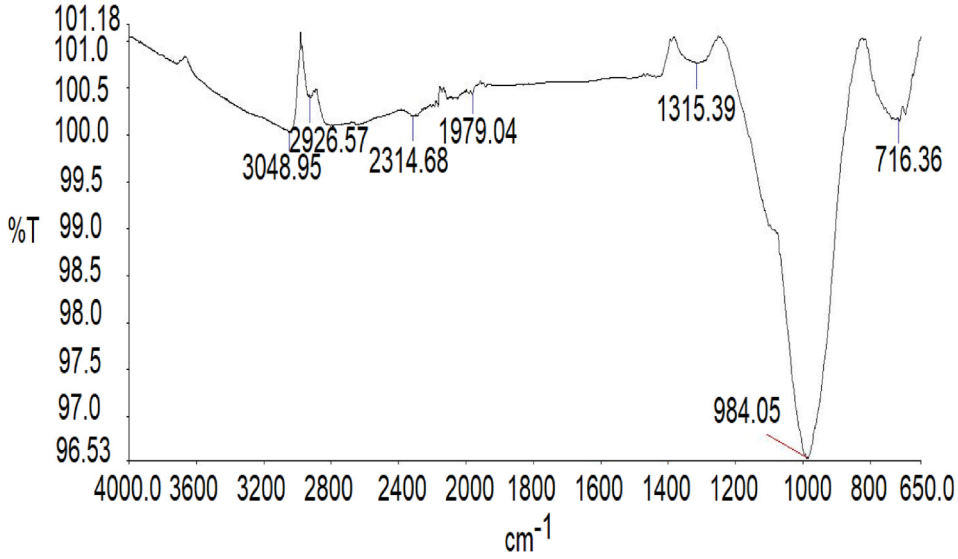

Fig. 26. FT-IR results of 10C + TBF sample after exposure to sulfuric acid over 3 months.

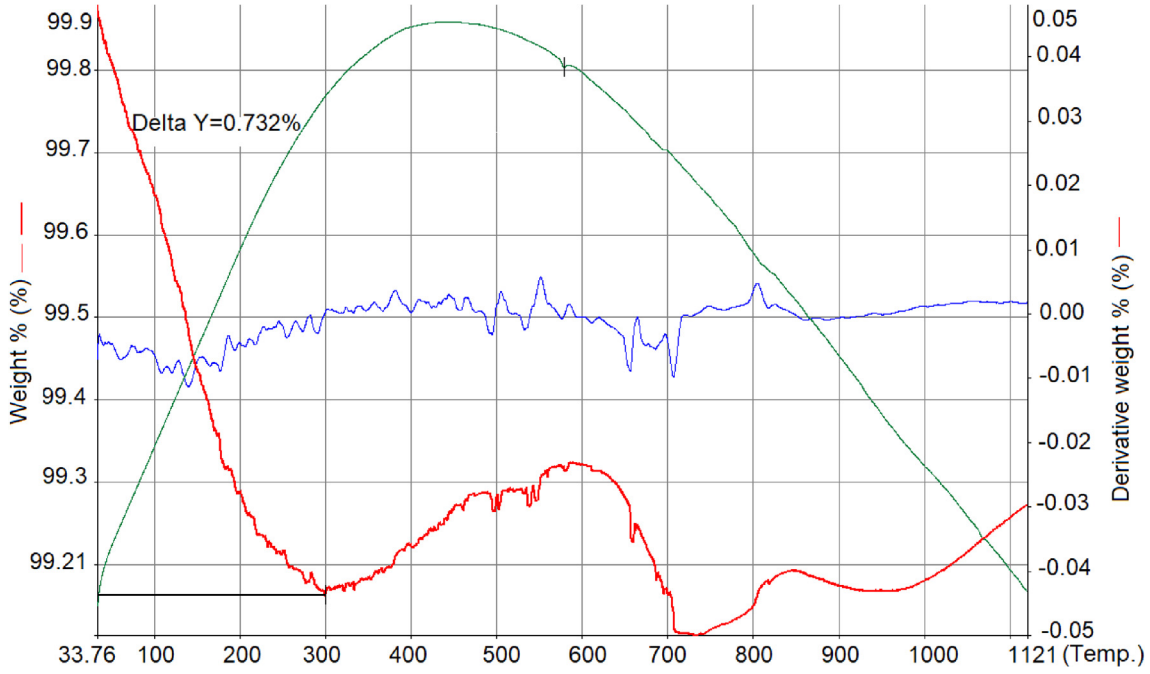

Fig. 27. TGA-DTA results of 10C + TBF after exposure to sulfuric acid over 3 months.

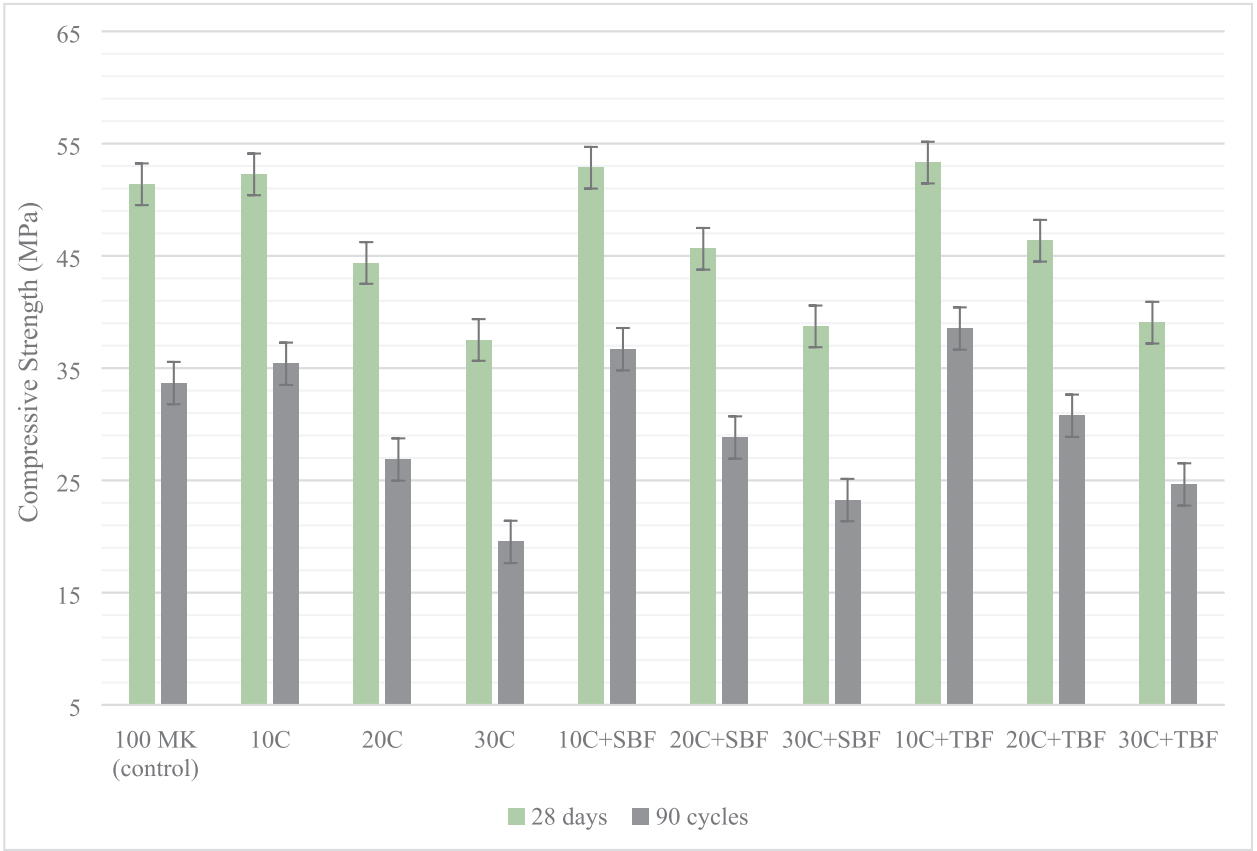

Fig. 28. Residual compressive strengths after the freezing-thawing test.

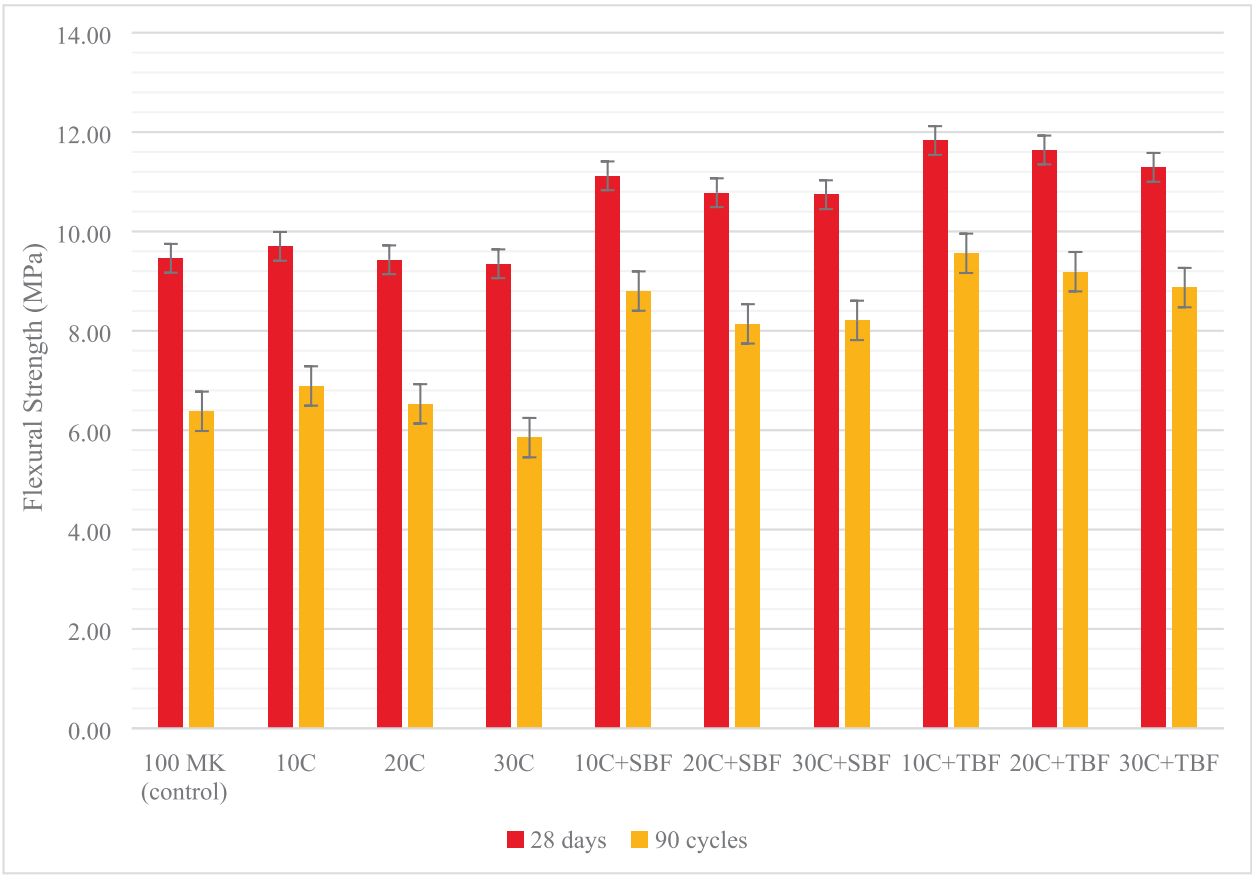

Fig. 29. Residual flexural strengths after the freezing-thawing test.

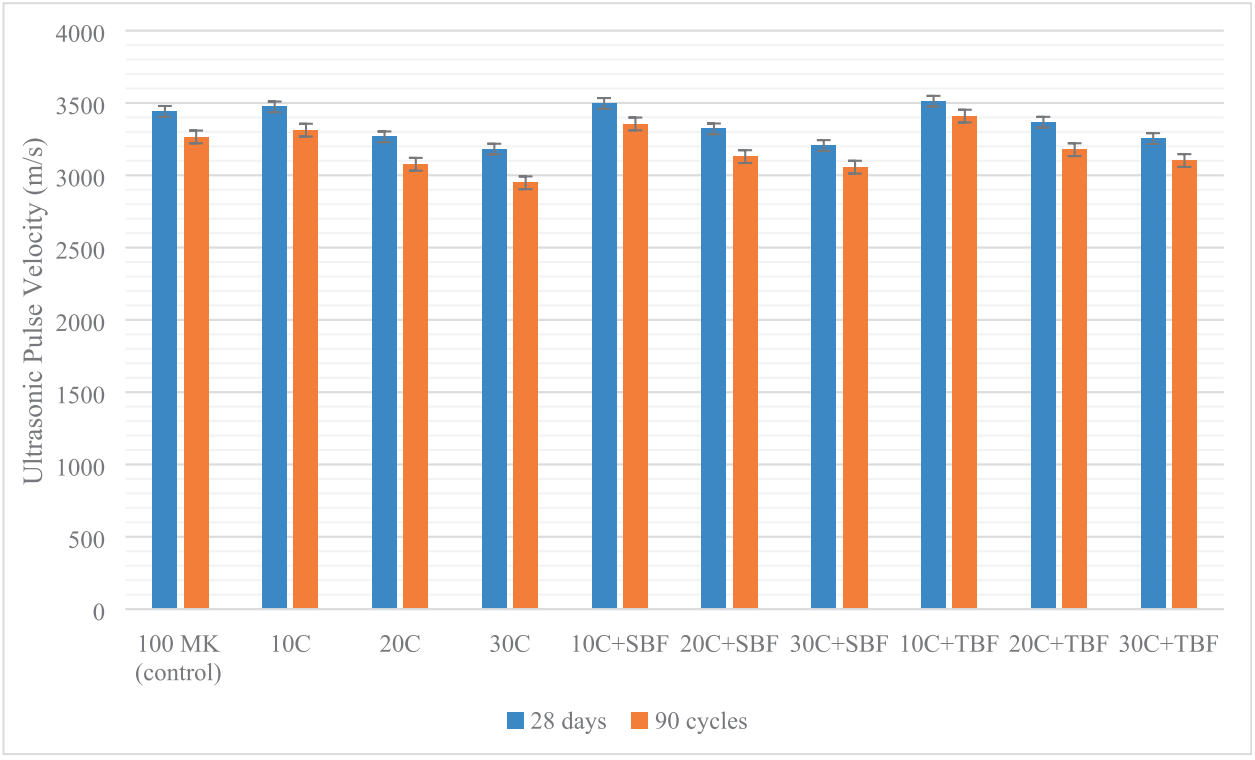

Fig. 30. UPV results after the freezing-thawing test.

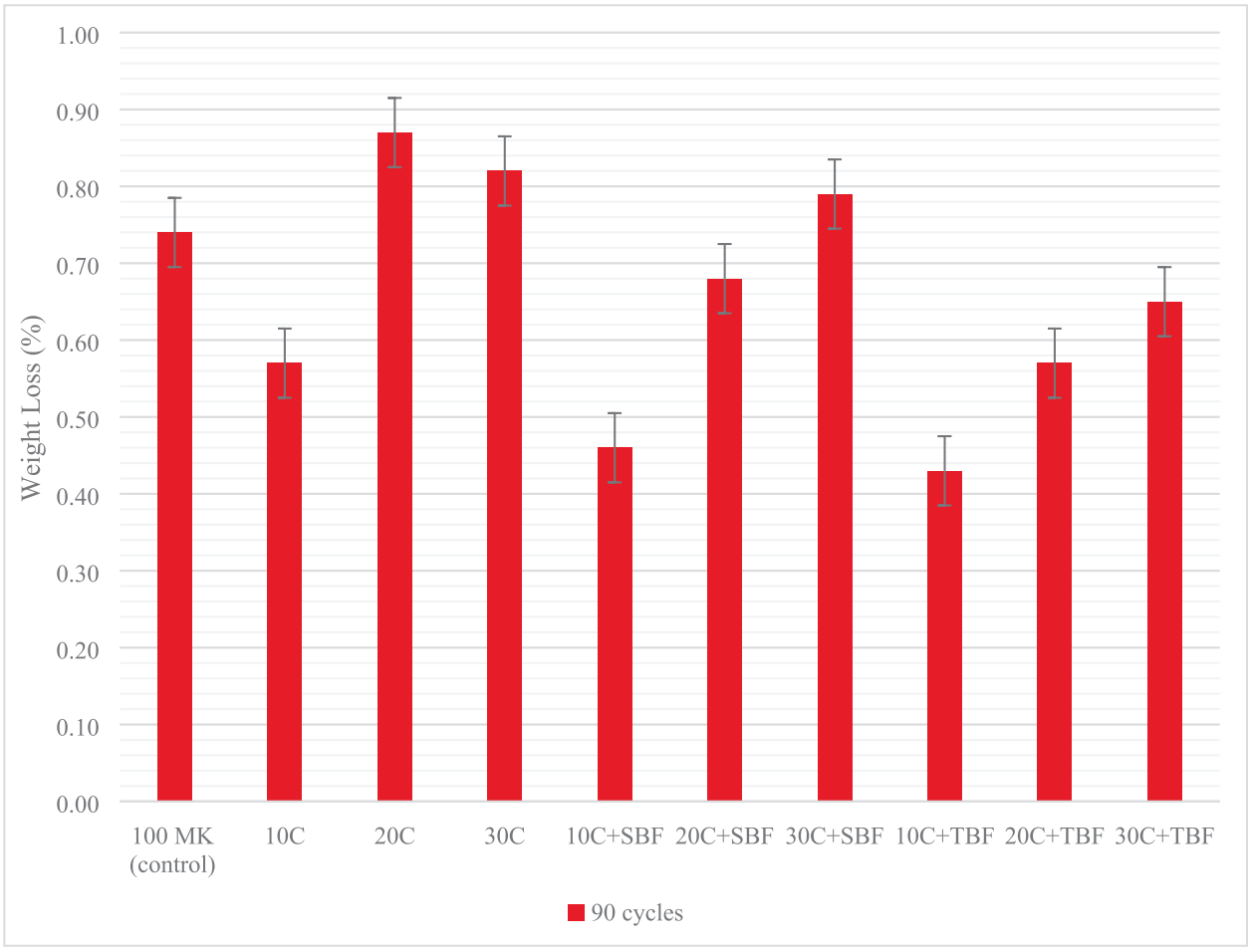

Fig. 31. Weight loss results after the freezing-thawing test.

Fig. 32. Visual inspection after the freezing-thawing test.

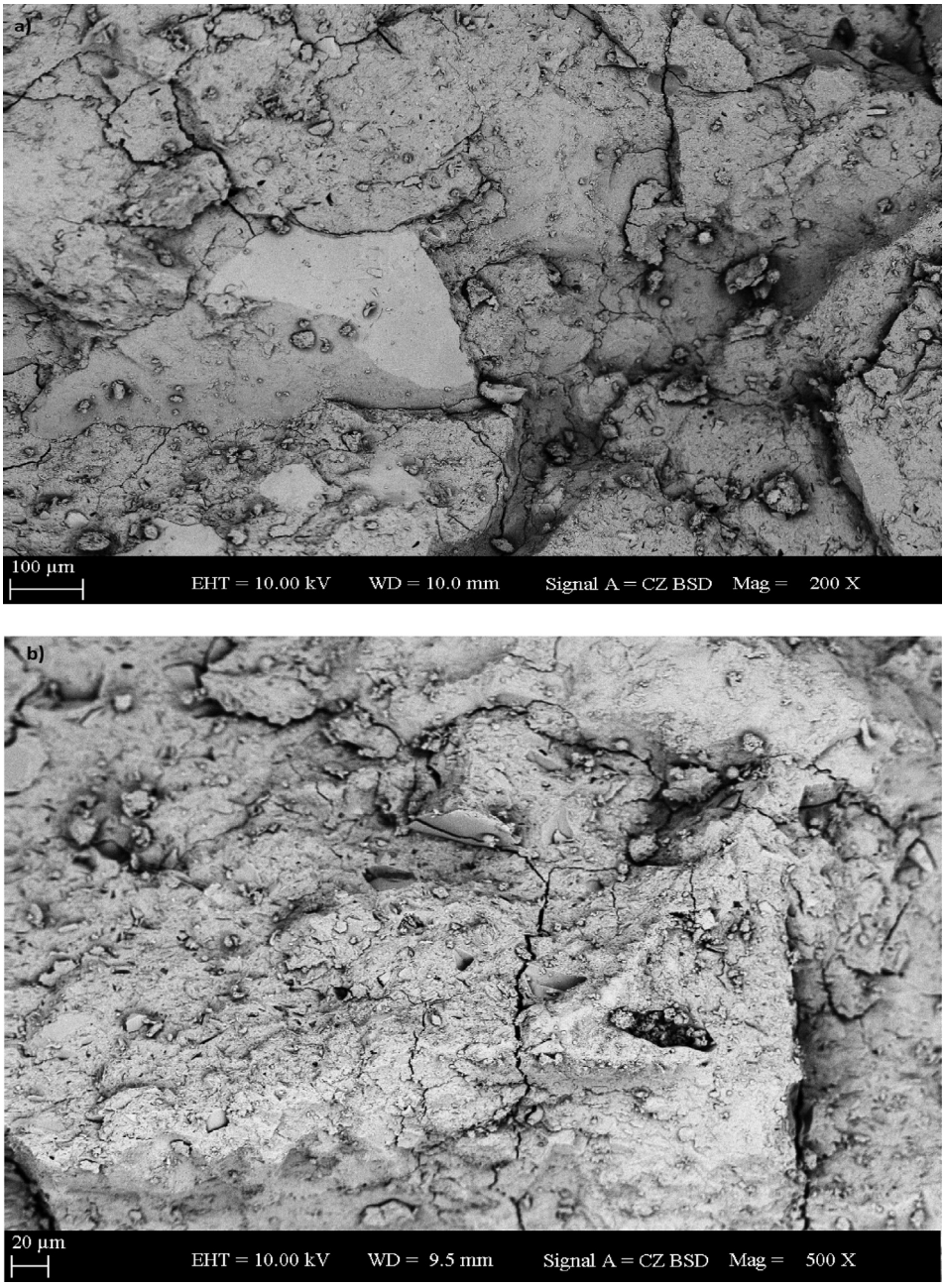

Fig. 33. SEM micrographs of 10C + TBF sample after the freezing-thawing test.

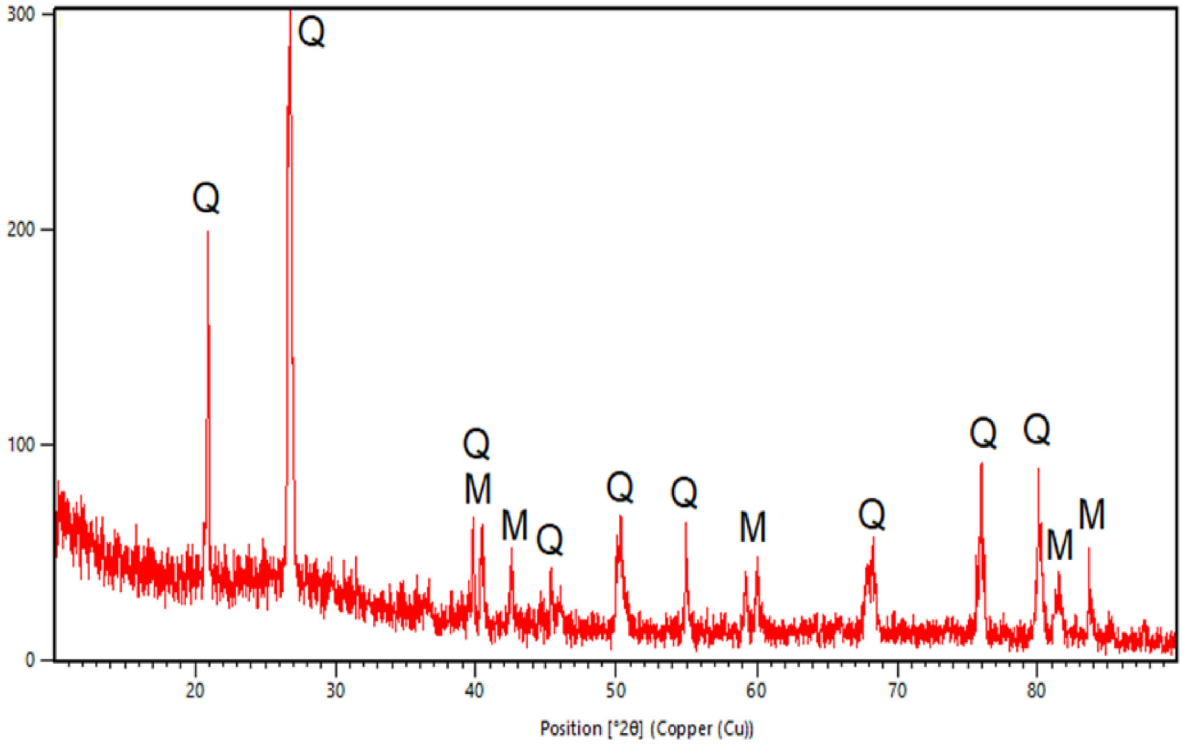

Fig. 34. XRD patterns of 10C + TBF sample after the freezing-thawing test.

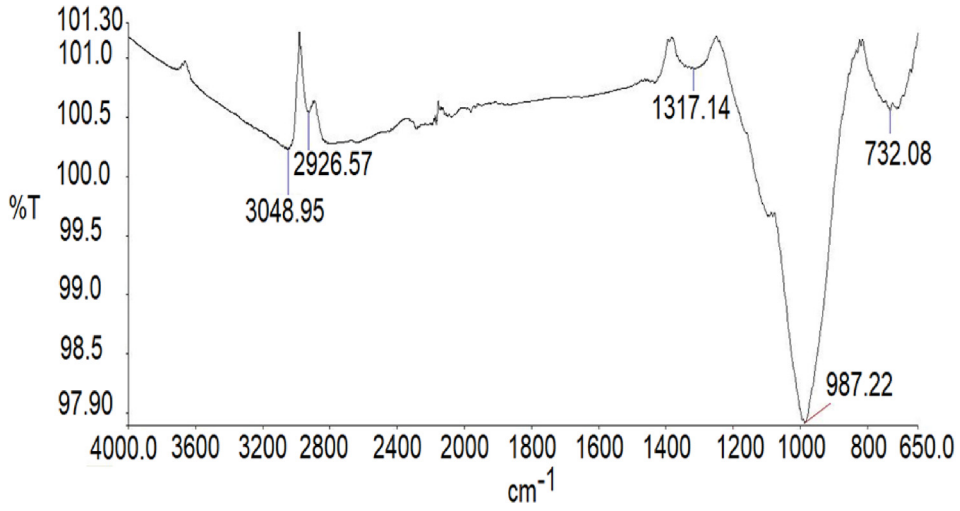

Fig. 35. FT-IR results of 10C + TBF specimen after the freezing-thawing test.

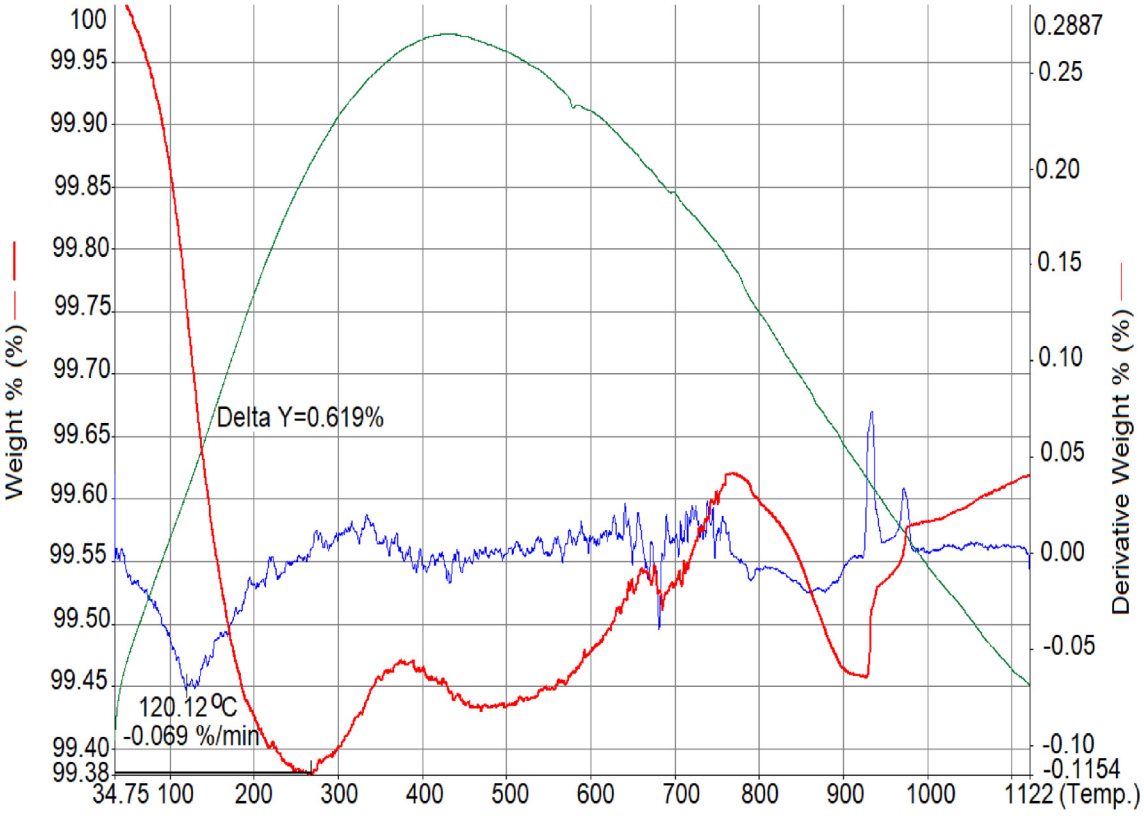

Fig. 36. TGA-DTA results of 10C + TBF specimen after the freezing-thawing test.

Declaration of Competing Interest

The authors declare that they have no known competing financial interests or personal relationships that could have appeared to influence the work reported in this paper.

Acknowledgment

This work was supported by the research fund of the Yildiz Technical University, the authors would like to express their sincere gratitude to scientific research coordination unit for their financial support to the project (Project number: FBA-2017-3081).

References

[1] P. Duxson, G.C. Lukey, J.S.J. Van Deventer, Physical evolution of Na-geopolymer derived from metakaolin up to 1000 °C, J. Mater. Sci. 42 (9) (2007) 3044–3054.
[2] C. Tippayasam, P. Balyore, P. Thavorniti, E. Kamseu, C. Leonelli, P. Chindaprasirt, D. Chaysuwan, Potassium alkali concentration and heat treatment affected metakaolin-based geopolymer, Constr. Build. Mater. 104 (2016) 293–297.
[3] T. Yang, H. Zhu, Z. Zhang, Influence of fly ash on the pore structure and shrinkage characteristics of metakaolin-based geopolymer pastes and mortars, Constr. Build. Mater. 153 (2017) 284–293.
[4] N. Belmokhtar, M. Ammari, J. Brigui, L. Ben allal, Comparison of the microstructure and the compressive strength of two geopolymers derived from Metakaolin and an industrial sludge, Constr. Build. Mater. 146 (2017) 621–629.
[5] J. Davidovits, Geopolymers - inorganic polymeric new materials, J. Therm. Anal. 37 (8) (1991) 1633–1656.
[6] G. Roviello, C. Menna, O. Tarallo, L. Ricciotti, C. Ferone, F. Colangelo, D. Asprone, R. Maggio, E. Cappelletto, A. Prota, R. Cioffi, Preparation, structure and properties of hybrid materials based on geopolymers and polysiloxanes, Mater. Des. 87 (2015) 82–94.
[7] W. Zhou, C. Yan, P. Duan, Y. Liu, Z. Zhang, X. Qiu, D. Li, A comparative study of high- and low-Al_2O_3 fly ash based-geopolymers: The role of mix proportion factors and curing temperature, Mater. Des. 95 (2016) 63–74.
[8] D. Rieger, T. Kovářík, J. Říha, R. Medlín, P. Novotný, P. Bělský, J. Kadlec, P. Holba, Effect of thermal treatment on reactivity and mechanical properties of alkali activated shale-slag binder, Constr. Build. Mater. 83 (2015) 26–33.
[9] L. Chen, Z. Wang, Y. Wang, J. Feng, Preparation and properties of alkali activated metakaolin-based geopolymer, Materials 9 (9) (2016) 1–12.
[10] H.K. Tchakouté, C.H. Rüscher, S. Kong, E. Kamseu, C. Leonelli, Geopolymer binders from metakaolin using sodium waterglass from waste glass and rice husk ash as alternative activators: a comparative study, Constr. Build. Mater. 114 (2016) 276–289.
[11] M. Gougazeh, Geopolymers from Jordanian metakaolin: Influence of chemical and mineralogical compositions on the development of mechanical properties, Jordan J. Civ. Engi. 7 (2) (2013) 236–257.
[12] P. Duan, C. Yan, W. Zhou, Influence of partial replacement of fly ash by metakaolin on mechanical properties and microstructure of fly ash geopolymer paste exposed to sulfate attack, Ceram. Int. 42 (2) (2016) 3504–3517.
[13] H. Wang, H. Li, F. Yan, Synthesis and mechanical properties of metakaolinite-based geopolymer, Colloids Surf., A 268 (1–3) (2005) 1–6.
[14] M.M. Al-mashhadani, O. Canpolat, Y. Aygörmez, M. Uysal, S. Erdem, Mechanical and microstructural characterization of fiber reinforced fly ash based geopolymer composites, Constr. Build. Mater. 167 (2018) 505–513.
[15] M.I.M. Alzeer, K.J.D. MacKenzie, R.A. Keyzers, Porous aluminosilicate inorganic polymers (geopolymers): a new class of environmentally benign heterogeneous solid acid catalysts, Appl. Catal. A 524 (2016) 173–181.
[16] E. Jamieson, B. McLellan, A. Van Riessen, H. Nikraz, Comparison of embodied energies of Ordinary Portland Cement with Bayer-derived geopolymer products, J. Cleaner Prod. 99 (2015) 112–118.
[17] Z. Li, S. Li, Carbonation resistance of fly ash and blast furnace slag based geopolymer concrete, Constr. Build. Mater. 163 (2018) 668–680.
[18] P. Duxson, J.L. Provis, G.C. Lukey, J.S.J. van Deventer, The role of inorganic polymer technology in the development of "green concrete", Cem. Concr. Res. 37 (12) (2007) 1590–1597.
[19] F. Pelisser, E.L. Guerrino, M. Menger, M.D. Michel, J.A. Labrincha, Micromechanical characterization of metakaolin-based geopolymers, Constr. Build. Mater. 49 (2013) 547–553.
[20] P. Rovnaník, Effect of curing temperature on the development of hard structure of metakaolin-based geopolymer, Constr. Build. Mater. 24 (7) (2010) 1176–1183.
[21] H.Y. Zhang, V. Kodur, S.L. Qi, L. Cao, B. Wu, Development of metakaolin-fly ash based geopolymers for fire resistance applications, Constr. Build. Mater. 55 (2014) 38–45.
[22] M. Lahoti, P. Narang, K.H. Tan, E. Yang, Mix design factors and strength prediction of metakaolin-based geopolymer, Ceram. Int. 43 (14) (2017) 11433–11441.

[23] Ü. Gemici, G. Tarcan, C. Helvacı, A.M. Somay, High arsenic and boron concentrations in groundwaters related to mining activity in the Bigadiç borate deposits (Western Turkey), Appl. Geochem. 23 (8) (2008) 2462–2476.
[24] U.K. Sevim, Colemanite ore waste concrete with low shrinkage and high split tensile strength, Mater. Struct. 44 (1) (2011) 187–193.
[25] O. Gencel, W. Brostow, C. Ozel, M. Filiz, An investigation on the concrete properties containing colemanite, Int. J. Phys. Sci. 5 (3) (2010) 216–225.
[26] I. Kula, A. Olgun, Y. Erdogan, V. Sevinc, Effects of colemanite waste, cool bottom ash, and fly ash on the properties of cement, Cem. Concr. Res. 31 (3) (2001) 491–494.
[27] M. Özdemir, N.U. Öztürk, Utilization of clay wastes containing boron as cement additives, Cem. Concr. Res. 33 (10) (2003) 1659–1661.
[28] J.N.Y. Djobo, A. Elimbi, H.K. Tchakouté, S. Kumar, Mechanical properties and durability of volcanic ash based geopolymer mortars, Constr. Build. Mater. J. 124 (2016) 606–614.
[29] M.A.M. Ariffin, M.A.R. Bhutta, M.W. Hussin, M. Mohd Tahir, N. Aziah, Sulfuric acid resistance of blended ash geopolymer concrete, Constr. Build. Mater. 43 (2013) 80–86.
[30] M. Zhang, M. Zhao, G. Zhang, D. Mann, K. Lumsden, M. Tao, Durability of red mud-fly ash based geopolymer and leaching behavior of heavy metals in sulfuric acid solutions and deionized water, Constr. Build. Mater. 124 (2016) 373–382.
[31] A. Mehta, R. Siddique, Sulfuric acid resistance of fly ash based geopolymer concrete, Constr. Build. Mater. 146 (2017) 136–143.
[32] D. Shen, W. Wang, Q. Li, P. Yao, G. Jiang, Early-age behaviour and cracking potential of fly ash concrete under restrained condition, Mag. Concr. Res. (2018) 1–16.
[33] Z. Yunsheng, S. Wei, L. Zongjin, Z. Xiangming, Z. Eddie, C. Chungkong, Impact properties of geopolymer based extrudates incorporated with fly ash and PVA short fiber, Constr. Build. Mater. 22 (3) (2008) 370–383.
[34] H. Assaedi, T. Alomayri, F.U.A. Shaikh, I.M. Low, Characterisation of mechanical and thermal properties in flax fabric reinforced geopolymer composites, J. Adv. Ceram. 4 (4) (2015) 272–281.
[35] P. Amuthakkannan, V. Manikandan, J.T.W. Jappes, M. Uthayakumar, Effect of fibre length and fibre content on mechanical properties of short basalt fibre reinforced polymer matrix composites, Mater. Phys. Mech. 16 (2013) 107–117.
[36] D. Shen, X. Liu, Q. Li, L. Sun, W. Wang, Early-age behavior and cracking resistance of high-strength concrete reinforced with Dramix 3D steel fiber, Constr. Build. Mater. 196 (2019) 307–316.
[37] L. Ricciotti, G. Roviello, O. Tarallo, F. Borbone, C. Ferone, F. Colangelo, M. Catauro, R. Cioffi, Synthesis and characterizations of melamine-based epoxy resins, Int. J. Mol. Sci. 14 (9) (2013) 18200–18214.
[38] P. Sun, H.C. Wu, Transition from brittle to ductile behavior of fly ash using PVA fibers, Cem. Concr. Compos. 30 (1) (2008) 29–36.
[39] K. Arunagiri, P. Elanchezhiyan, V. Marimuthu, G. Arunkumar, P. Rajeswaran, Mechanical properties of basalt fiber based geopolymer concrete, Int. J. Sci., Eng. Technol. Res. 6 (4) (2017) 551–556.
[40] D. Shen, C. Li, Z. Feng, C. Wen, B. Ojha, Influence of strain rate on bond behavior of concrete members reinforced with basalt fiber-reinforced polymer rebars, Constr. Build. Mater. 228 (2019) 116755.
[41] G. Görhan, R. Aslaner, O. Şinik, The effect of curing on the properties of metakaolin and fly ash-based geopolymer paste, Compos. B Eng. 97 (2016) 329–335.
[42] Y.M. Liew, C.Y. Heah, L. Yuan Li, N.A. Jaya, M.M.A.B. Abdullah, S.J. Tan, K. Hussin, Formation of one-part-mixing geopolymers and geopolymer ceramics from geopolymer powder, Constr. Build. Mater. 156 (2017) 9–18.
[43] K. Kaya, S. Soyer-Uzun, Evolution of structural characteristics and compressive strength in red mud-metakaolin based geopolymer systems, Ceram. Int. 42 (6) (2016) 7406–7413.
[44] A. Sabbatini, L. Vidal, C. Pettinari, I. Sobrados, S. Rossignol, Control of shaping and thermal resistance of metakaolin-based geopolymers, Mater. Des. 116 (2017) 374–385.
[45] O.G. Rivera, W.R. Long, C.A. Weiss, R.D. Moser, B.A. Williams, K. Torres-Cancel, E.R. Gore, P.G. Allison, Effect of elevated temperature on alkali-activated geopolymeric binders compared to portland cement-based binders, Cem. Concr. Res. 90 (2016) 43–51.
[46] M. Uysal, M.M. Al-mashhadani, Y. Aygörmez, O. Canpolat, Effect of using colemanite waste and silica fume as partial replacement on the performance of metakaolin-based geopolymer mortars, Constr. Build. Mater. 176 (2018) 271–282.
[47] A. Celik, K. Yilmaz, O. Canpolat, M.M. Al-mashhadani, Y. Aygörmez, M. Uysal, High-temperature behavior and mechanical characteristics of boron waste additive metakaolin based geopolymer composites reinforced with synthetic fibers, Constr. Build. Mater. 187 (2018) 1190–1203.
[48] ASTM C109/109M, Standard Test Method for Compressive Strength of Hydraulic Cement Mortars (Using 2-in. or [50-mm] Cube Specimens) 1. Chemical Analysis, (C109/C109M – 11b), 2010, 1–9.
[49] ASTM C348, Standard Test Method for Flexural Strength of Hydraulic-Cement Mortars ASTM C348, Annual Book of ASTM Standards, 4, 1998, 2–7.
[50] ASTM C944/C944 M, ASTEM C944/C944M - 12 - Standard Test Method for Abrasion Resistance of Concrete or Mortar Surfaces by the Rotating-Cutter Method, ASTM International, 2012, 1–5.
[51] A. Olgun, T. Kavas, Y. Erdogan, G. Once, Physico-chemical characteristics of chemically activated cement containing boron, Build. Environ. 42 (2007) 2384–2395.
[52] Y. Erdogan, M.S. Zeybek, A. Demirbaş, Cement mixes containing colemanite from concentrator wastes, Cem. Concr. Res. 28 (4) (1998) 605–609.
[53] S. Elshafie, M. Boulbibane, G.S. Whittleston, Mechanical performance of reinforced concrete with different proportions and lengths of Basalt Fibres, J. Mater. Sci. Eng. 5 (2016) 1–9.
[54] O. Kayali, M.N. Haque, B. Zhu, Some characteristics of high strength fiber reinforced lightweight aggregate concrete, Cem. Concr. Compos. 25 (2003) 207–213.
[55] R.F. Zollo, Fiber-reinforced concrete: an overview after 30 years of development, Cem. Concr. Compos. 19 (1997) 107–122.
[56] P.P. Palchik, On control testing of fiber-concrete samples to determine their compression and tensile strength at bending, Kyiv National University of Construction and Architecture Protocol No 64-1-11, 2011.
[57] J. Ma, X. Qiu, L. Cheng, Y. Wang, Experimental research on the fundamental mechanical properties of presoaked basalt fiber concrete, Adv. FRP Compos. Civ. Eng. (2010) 85–88.
[58] A.M. Neville, Properties of Concrete, in: Longman Science and Technology, Longman Group, Longman House, Essex, England, 1987.
[59] T.M. Borhan, Thermal and mechanical properties of basalt fibre reinforced concrete, World Acad. Sci., Eng. Technol. 7 (2013) 712–715.
[60] N. Kabay, Abrasion resistance and fracture energy of concretes with basalt fiber, Constr. Build. Mater. 50 (2014) 95–101.
[61] Y.J. Zhang, S. Li, Y.C. Wang, D.L. Xu, Microstructural and strength evolutions of geopolymer composite reinforced by resin exposed to elevated temperature, J. Non-Cryst. Solids 358 (3) (2012) 620–624.
[62] H.Y. Zhang, V. Kodur, P.E., ASCE, F., B. Wu, L. Cao, Liang, S. Qi, Comparative thermal and mechanical performance of geopolymers derived from metakaolin and fly ash, J. Mater. Civ. Eng. 28 (2) (2016) 1–12.
[63] S. Yilmaz, O.T. Ozkan, V. Gunay, Crystallization kinetics of basalt glass, Ceram. Int. 22 (1996) 477–481.
[64] J. Sim, C. Park, D.Y. Moon, Characteristics of basalt fiber as a strengthening material for concrete structures, Compos. B 36 (2005) 504–512.
[65] D.L.Y. Kong, J.G. Sanjayan, K.S. Crentsil, Comparative performance of geopolymers made with metakaolin and fly ash after exposure to elevated temperatures, Cem. Concr. Res. 37 (2007) 1583–1589.
[66] A. Natali, S. Manzi, M.C. Bignozzi, Novel fibre reinforced composite materials based on sustainable geopolymer matrix, 21 (2011) 1124–1131.
[67] I.B. Topçu, C. Karakurt, Properties of reinforced concrete steel rebars exposed to high temperatures, Adv. Mater. Sci. Eng. (2008). 2008(September 2001).
[68] D.L.Y. Kong, J.G. Sanjayan, K. Sagoe-Crentsil, Comparative performance of geopolymers made with metakaolin and fly ash after exposure to elevated temperatures, Cem. Concr. Res. 37 (12) (2007) 1583–1589.
[69] P. He, D. Jia, T. Lin, M. Wang, Y. Zhou, Effects of high-temperature heat treatment on the mechanical properties of unidirectional carbon fiber reinforced geopolymer composites, Ceram. Int. 36 (2010) 1447–1453.
[70] P. Behera, V. Baheti, J. Militky, P. Louda, Elevated temperature properties of basalt microfibril filled geopolymer composites, Constr. Build. Mater. 163 (2018) 850–860.
[71] M. Lahoti, K.K. Wong, E. Yang, K.H. Tan, Effects of Si/Al molar ratio on strength endurance and volume stability of metakaolin geopolymers subject to elevated temperature, Ceram. Int. 44 (2018) 5726–5734.
[72] S. Louati, Z. Fakhfakh, H. Douiri, M. Arous, S. Baklouti, Enhanced dielectric performance of metakaolin–H 3 PO 4 geopolymers, Mater. Lett. 164 (2015) 299–302.
[73] R.R. de S. Guerra, T. da S. Rocha, D.P. Dias, L.R. da C. de O. Marques, F.C.C. França, Metakaolin-based geopolymer mortars with different alkaline activators (Na + and K +), Constr. Build. Mater. 178 (2018) 453–461.
[74] F.N. Degirmenci, Freeze-thaw and fire resistance of geopolymer mortar based on natural and waste pozzolans, Ceramics-Silikáty 62 (1) (2018) 41–49.
[75] R. Slavik, V. Bednarik, M. Vondruska, A. Nemec, Preparation of geopolymer from fluidized bed combustion bottom ash, J. Mater. Process. Technol. (2007) 265–270.
[76] L.Y. Gomez-Zamorano, E. Vega-Cordero, L. Struble, Composite geopolymers of metakaolin and geothermal nanosilica waste, Constr. Build. Mater. 115 (2016) 269–276.
[77] T. Bakharev, Resistance of geopolymer materials to acid attack, Cem. Concr. Res. 35 (2005) 658–670.
[78] M. Criado, A. Fernández-jiménez, A.G. De Torre, M.A.G. Aranda, A. Palomo, An XRD study of the effect of the SiO_2 / Na_2O ratio on the alkali activation of fly ash, Cem. Concr. Res. 37 (2007) 671–679.
[79] K. Bouguermouh, N. Bouzidi, L. Mahtout, L. Pérez-villarejo, M.L. Martínez-cartas, Effect of acid attack on microstructure and composition of metakaolinbased geopolymers: The role of alkaline activator, J. Non-Cryst. Solids 463 (2017) 128–137.
[80] S. Pilehvar, A.M. Szczotok, J.F. Rodríguez, L. Valentini, M. Lanzón, R. Pamies, A.L. Kjøniksen, Effect of freeze-thaw cycles on the mechanical behavior of geopolymer concrete and Portland cement concrete containing micro-encapsulatedphase change materials, Constr. Build. Mater. 200 (2019) 94–103.
[81] A. Allahverdi, M.M.B.R. Abadi, K.M. Anwar Hossain, M. Lachemi, Resistance of chemically-activated high phosphorous slag content cement against freeze–thaw cycles, Cold Regions Sci. Technol., 103 (Supplement C) (2014) 107–114.
[82] L. Basheer, J. Kropp, D.J. Cleland, Assessment of the durability of concrete from its permeation properties: a review, Constr. Build. Mater. 15 (2) (2001) 93–103.
[83] P. Sun, H.-C. Wu, Chemical and freeze–thaw resistance of fly ash-based inorganic mortars, Fuel 111 (2013) 740–745.